



# Construction of Energy Preserving QMF

Jian-ao Lian<sup>†</sup> & Yonghui Wang<sup>‡</sup>

Department of {Mathematics<sup>†</sup>, Engineering Technology<sup>‡</sup>}  
Prairie View A&M University  
Prairie View, TX 77446-0519 USA  
e-mail: {[jjilian](mailto:jjilian@pvamu.edu), [yowang](mailto:yowang@pvamu.edu)}@pvamu.edu

Received February 6, 2016; accepted May 9, 2016

## Abstract

Recently, a family of perfect reconstruction (PR) quadrature mirror filterbanks (QMF) with finite impulse response filters (FIR) from systems of biorthogonal refinable functions and wavelets were introduced and also applied to image processing. However, a detailed procedure was absent. The main objective of this paper is to present extensive examples that will provide a thorough process of construction of the new family of PR QMF with FIR filterbanks. These new filters are linear-phase due to the symmetry property of their corresponding biorthogonal refinable functions and wavelets. In addition, these filters have odd lengths so that the symmetric extension can be easily applied. Another important feature is that the filters preserve energy (EP) very well. The notion of Condition EP was thus introduced for the purpose of further examining these features.

**Key Words:** biorthogonality; energy preservation; quadrature mirror filterbank; wavelets

**MSC 2010 No.:** 42C40; 65T60; 68U10; 94A08

## 1. Introduction

SUBBAND image coders require high performance filterbanks. A family of these high-performance filterbanks can be created from *biorthogonal* pairs of refinable functions and wavelets. Contrary to the orthonormal wavelets (Daubechies, 1988), it is well-known that one of the major advantages of the compactly supported biorthogonal wavelets is its symmetry (Le Gall and Tabatabai, 1988; Cohen et al., 1992), (Daubechies, 1992, p.259). The symmetry property, in turn, implies the existence of the linear-phase finite impulse response (FIR) lowpass and highpass

perfect reconstruction (PR) quadrature mirror filters (QMF), which originate from the symmetry of the underlying compactly supported refinable functions and wavelets. To avoid artifacts along image boundaries when an image coder is applied, odd length filterbanks (FB) are desired so that the symmetric extension can be easily applied. Moreover, wavelet subbands' *energy* on consecutive decomposition levels need to be relatively well *preserved*, where the energy of wavelet coefficients is determined by the *weights* of the biorthogonal filterbanks (BFB). Here, weights of a system of BFB is defined in Section 3 by the  $\ell_2$ -norm squares of the lowpass and highpass filters. Certainly, filterbanks from orthonormal wavelets have perfect energy preservation, namely, their  $\ell_2$ -norm squares are always one. However, filterbanks from biorthogonal wavelets are generally not (Woods and Naveen, 1992; Usevitch, 1996; Usevitch, 2001). This criterion of determining their performance can be defined by how close they are to filterbanks from orthonormal wavelets. In other words, a pair of biorthogonal refinable function and wavelet is *good* only if they are *near orthonormal*. Or, equivalently and more specifically, their weights must be as close to one as possible.

For convenience, filterbanks  $(\mathbf{h}, \mathbf{g})$ , with lowpass filter  $\mathbf{h} = \{h_k\}_{k \in \mathbb{Z}}$  and highpass filter  $\mathbf{g} = \{g_k\}_{k \in \mathbb{Z}}$ , are said to be *energy-preserving*, denoted by Condition EP, if their  $L_2$  norms are close to 1, i.e.,  $\|\mathbf{h}\|_2 \approx 1$  and  $\|\mathbf{g}\|_2 \approx 1$ , with the  $\ell_2$ -norm of  $\mathbf{h}$ , e.g., defined by  $\|\mathbf{h}\|_2^2 = \sum_{k \in \mathbb{Z}} |h_k|^2$ . To be more specific, Conditions EP1–EP4 are introduced if both  $\|\mathbf{h}\|_2$  and  $\|\mathbf{g}\|_2$  satisfy one of the following conditions:

$$\textbf{Condition EP1: } \|\mathbf{h}\|_2 = 1, \quad \left| \|\mathbf{g}\|_2^2 - 1 \right| = \text{the smallest}; \quad (1)$$

$$\textbf{Condition EP2: } \|\mathbf{g}\|_2 = 1, \quad \left| \|\mathbf{h}\|_2^2 - 1 \right| = \text{the smallest}; \quad (2)$$

$$\textbf{Condition EP3: } \|\mathbf{h}\|_2 = \|\mathbf{g}\|_2, \quad \left| \|\mathbf{h}\|_2^2 - 1 \right| = \text{the smallest}; \quad (3)$$

$$\textbf{Condition EP4: } \left( \|\mathbf{h}\|_2^2 - 1 \right)^2 + \left( \|\mathbf{g}\|_2^2 - 1 \right)^2 = \text{the smallest}. \quad (4)$$

JPEG 2000, the new image compression standard, uses the biorthogonal 5/3, called LeGall 5/3 (Le Gall and Tabatabai, 1988) for lossless compression. It is also referred to as Cohen-Daubechies-Feauveau (CDF) wavelet filters (Cohen et al., 1992), or CDF 5/3 for short. For lossy compression, JPEG 2000 uses the biorthogonal wavelet filters CDF 9/7 (Cohen et al., 1992). Notice that both LeGall 5/3 and CDF 9/7 do not satisfy any of the four specific EP conditions in (1)–(4). However, as we will see at the end of Section IV, CDF 9/7 does feature the energy-preserving property very well, though LeGall 5/3 does not preserve energy well enough.

New filterbanks in this paper feature all of the above listed properties, with Condition EP in particular. Some of our results in this paper were successfully applied to image processing (Lian and Wang, 2014). However, a detailed construction of the new family of biorthogonal PR FIR QMF was not provided in (Lian and Wang, 2014). Henceforward, the main purpose of this paper is to furnish more specifics or fill the gaps of the construction.

To facilitate presentation, some background information or preliminaries and literature review are given in Section 2. Following (Woods and Naveen, 1992; Usevitch, 1996; Usevitch, 2001), weights are re-defined and re-formulated in terms of two-scale sequences by convolution in Section 3. A convenient algorithm of how to build up a system of biorthogonal wavelets constitutes Section 4.

A new family of biorthogonal refinable functions and wavelets, and consequently, BFBs with certain Condition EP's, are constructed in Section 5. Smoothness of the new biorthogonal refinable functions and wavelets are analyzed in Section 6. We demonstrate our new BFBs in Section 7. by applying them to image compression and image denoising. Some concluding remarks and discussions are found in Section 8. An efficient algorithm for evaluating the Riesz bounds by using Euler-Frobenius polynomials is illustrated in Appendix I. In addition, for completeness, some additional BFBs with certain EP conditions, including 7/5, 9/7, 11/9, and 13/11, are provided in the Appendix II, while the even-length BFBs with Condition EP3 are discussed in Appendix III.

## 2. Background

It is well-known that under appropriate normalization conditions, a pair of compactly supported *refinable function*  $\phi$  and *eavelet*  $\psi$  are determined by functional equations

$$\phi(t) = \sqrt{2} \sum_{k \in \mathbb{Z}} h_k \phi(2t - k), \quad (5)$$

$$\psi(t) = \sqrt{2} \sum_{k \in \mathbb{Z}} g_k \phi(2t - k), \quad t \in \mathbb{R}, \quad (6)$$

where both  $\{\sqrt{2}h_k\}_{k \in \mathbb{Z}}$  and  $\{\sqrt{2}g_k\}_{k \in \mathbb{Z}}$  have finite nonzero entries and are called the *two-scale sequences* of  $\phi$  and  $\psi$ . The functional equations (5) and (6) are referred to as the *two-scale relations* of  $\phi$  and  $\psi$ . In terms of Fourier transforms, the functional equations (5) and (6) determining such a wavelet system  $(\phi, \psi)$  are equivalent to

$$\widehat{\phi}(\omega) = H(z) \widehat{\phi}\left(\frac{\omega}{2}\right), \quad (7)$$

$$H(z) = \frac{1}{\sqrt{2}} \sum_{k \in \mathbb{Z}} h_k z^k; \quad (8)$$

$$\widehat{\psi}(\omega) = G(z) \widehat{\phi}\left(\frac{\omega}{2}\right), \quad (9)$$

$$G(z) = \frac{1}{\sqrt{2}} \sum_{k \in \mathbb{Z}} g_k z^k, \quad (10)$$

where  $z = \exp(-j\omega/2)$ ,  $j = \sqrt{-1}$ ;  $H$  and  $G$  are the *two-scale symbols* of  $\phi$  and  $\psi$ , respectively. In signal and image processing,  $\{h_k\}_{k \in \mathbb{Z}}$  in (5) or (8) is used for the lowpass filter, and  $\{g_k\}_{k \in \mathbb{Z}}$  in (6) or (10) is for the highpass filter. With  $H$  and  $G$  in (7)–(10), a square polynomial matrix  $M_{H,G}$  of order 2 is introduced as

$$M_{H,G}(z) = \begin{bmatrix} H(z) & H(-z) \\ G(z) & G(-z) \end{bmatrix}. \quad (11)$$

For all QMF filters  $(\{h_k\}_{k \in \mathbb{Z}}, \{g_k\}_{k \in \mathbb{Z}})$  to be with FIR, it is natural to require that

$$\det(M_{H,G}(z)) = \varepsilon z^{2K-1}, \quad |z| = 1, \quad (12)$$

for some integer  $K$ , where  $\varepsilon = 1$  or  $-1$ . Under the condition (12), a new wavelet system  $(\widetilde{\phi}, \widetilde{\psi})$  can be established, which is *dual* or *biorthogonal* to  $(\phi, \psi)$ . Analogous to (7)–(10) for  $(\phi, \psi)$ ,

the biorthogonal wavelet system  $(\tilde{\phi}, \tilde{\psi})$  can also be formulated by

$$\widehat{\tilde{\phi}}(\omega) = \tilde{H}(z) \widehat{\phi}\left(\frac{\omega}{2}\right), \quad (13)$$

$$\tilde{H}(z) = \frac{1}{\sqrt{2}} \sum_{k \in \mathbb{Z}} \tilde{h}_k z^k; \quad (14)$$

$$\widehat{\tilde{\psi}}(\omega) = \tilde{G}(z) \widehat{\phi}\left(\frac{\omega}{2}\right), \quad (15)$$

$$\tilde{G}(z) = \frac{1}{\sqrt{2}} \sum_{k \in \mathbb{Z}} \tilde{g}_k z^k, \quad (16)$$

with  $\tilde{H}$  and  $\tilde{G}$  being the two-scale symbols of  $\tilde{\phi}$  and  $\tilde{\psi}$ ,  $\{\sqrt{2}\tilde{h}_k\}_{k \in \mathbb{Z}}$  and  $\{\sqrt{2}\tilde{g}_k\}_{k \in \mathbb{Z}}$  the two-scale sequences of  $\tilde{\phi}$  and  $\tilde{\psi}$ . The biorthogonality conditions between the wavelet system  $(\phi, \psi)$  and its dual  $(\tilde{\phi}, \tilde{\psi})$  are governed and reflected by the fact that  $M_{\tilde{H}, \tilde{G}}(z)$  is the inverse of  $M_{H, G}(z)^*$  on  $|z| = 1$ , namely,

$$M_{\tilde{H}, \tilde{G}}(z) M_{H, G}(z)^* = I_2, \quad |z| = 1, \quad (17)$$

where  $\star$  denotes the complex conjugation of the transpose, and  $I_2$  is the identity matrix of order 2.

With the natural requirement (12),  $G$  and  $\tilde{G}$  can be obtained from  $H$  and  $\tilde{H}$  directly from the matrix identity (17):

$$G(z) = -\varepsilon z^{2K-1} \overline{\tilde{H}(-z)}, \quad (18)$$

$$\tilde{G}(z) = -\varepsilon z^{2K-1} \overline{H(-z)}, \quad (19)$$

with  $H$  and  $\tilde{H}$  satisfying

$$H(z) \overline{\tilde{H}(z)} + H(-z) \overline{\tilde{H}(-z)} = 1, \quad |z| = 1. \quad (20)$$

In other words, a complete biorthogonal wavelet system, denoted by, e.g.,  $(\phi, \psi)$  and  $(\tilde{\phi}, \tilde{\psi})$ , is completely determined if  $H$  and  $\tilde{H}$  are determined through the identity (20). For instance, for LeGall 5/3,  $\varepsilon = -1$  and  $K = 2$  in (12), and and brusque calculation yields

$$H(z) = \frac{1}{2} \left( \frac{1+z}{2} \right)^2 (-1 + 4z - z^2), \quad (21)$$

$$\tilde{H}(z) = z \left( \frac{1+z}{2} \right)^2. \quad (22)$$

For CDF 9/7,  $\varepsilon = -1$  and  $K = 4$  in (12), and

$$H(z) = \left( \frac{1+z}{2} \right)^4 (s_0 + s_1 z + (1 - 2s_0 - 2s_1)z^2 + s_1 z^3 + s_0 z^4), \quad (23)$$

$$\tilde{H}(z) = z \left( \frac{1+z}{2} \right)^4 (\tilde{s}_0 + (1 - 2\tilde{s}_0)z + \tilde{s}_0 z^2), \quad (24)$$

where

$$s_0 = \frac{1}{336} \left( 70 - 7(5 - \sqrt{15})\alpha + (2\sqrt{15} - 5)\alpha^2 \right), \quad (25)$$

$$s_1 = \frac{1}{24} \left( -36 + 2(6 - \sqrt{15})\alpha - (\sqrt{15} - 3)\alpha^2 \right), \quad (26)$$

$$\tilde{s}_0 = -\frac{1}{168} \left( 56 + 14\alpha - (3\sqrt{15} - 11)\alpha^2 \right), \quad (27)$$

with

$$\alpha = \sqrt[3]{154 + 42\sqrt{15}}. \quad (28)$$

In the wavelet literature, although there is no clear standard for BFB's energy preservation or energy compaction measure, there are some studies regarding the energy preservation or compaction of biorthogonal filterbanks (cf., e.g., (Wei et al., 1998; Yang et al., 1998; Abdelnour and Selesnick, 2004; de Saint-Martin et al., 1999)). Due to the fact that  $|H(z)|^2 + |H(-z)|^2 = 1$  on  $|z| = 1$  is necessary if  $H$  is the two-scale symbol of an orthonormal refinable function, Cohen et al. (Cohen et al., 1992) and Daubechies (Daubechies, 1992, p.283) used the method of minimizing

$$\left| \int_{-\pi}^{\pi} [1 - |H(e^{-j\omega})|^2 - |H(-e^{-j\omega})|^2] d\omega \right|, \quad (29)$$

to obtain  $H$  first then established  $\tilde{H}$  afterward. In fact, for any two-scale symbol  $H$  in (8) and  $\tilde{H}$  in (14),

$$\frac{1}{2\pi} \int_{-\pi}^{\pi} [1 - |H(e^{-j\omega})|^2 - |H(-e^{-j\omega})|^2] d\omega = 1 - \sum_{k \in \mathbb{Z}} h_k^2, \quad (30)$$

$$\frac{1}{2\pi} \int_{-\pi}^{\pi} [1 - |\tilde{H}(e^{-j\omega})|^2 - |\tilde{H}(-e^{-j\omega})|^2] d\omega = 1 - \sum_{k \in \mathbb{Z}} \tilde{h}_k^2. \quad (31)$$

Hence,  $\|\mathbf{h}\|_2^2 = 1$  in (1) for Condition EP1 is equivalent to allowing the integral on the left of (30) to be zero;  $\|\tilde{\mathbf{g}}\|_2^2 = 1$  in (2) for Condition EP2 is equivalent to allowing the integral for  $\tilde{H}$  on the left of (31) to be zero due to (18).

Wei et al. (Wei et al., 1998) constructed a family of general biorthogonal coifman wavelet systems (GBCW) where the energy compaction capability was also concerned but not considered during the filter construction. As an example, the GBCW 9/7 in (Wei et al., 1998) was

$$\mathbf{h} = \{h_k\}_{k=0,\dots,8} = \frac{1}{32\sqrt{2}} \{1, 0, -8, 16, 46, 16, -8, 0, 1\},$$

$$\tilde{\mathbf{h}} = \{\tilde{h}_k\}_{k=1,\dots,7} = \frac{1}{16\sqrt{2}} \{-1, 0, 9, 16, 9, 0, -1\}.$$

However,

$$\|\mathbf{h}\|_2^2 = \frac{1379}{1024} = 1.3466796875,$$

$$\|\tilde{\mathbf{h}}\|_2^2 = \frac{105}{128} = .8203125,$$

both relatively away from one.

Yang et al. (Yang et al., 1998) designed PR biorthogonal filterbanks that maximize orthonormality subject to adjustable structural constraints in order to achieve various degrees of energy compaction.

Due to the necessary conditions

$$\sum_{k \in \mathbb{Z}} h_k h_{k+2\ell} = \delta_{\ell,0}, \quad \ell \in \mathbb{Z}, \quad (32)$$

for an orthogonal filter  $\{h_k\}_{k \in \mathbb{Z}}$ , Abdelnour and Selesnick (Abdelnour and Selesnick, 2004) introduced the angles among all even-integer shifts of a lowpass filter  $\{h_k\}_{k \in \mathbb{Z}}$  and then constructed symmetric nearly orthogonal biorthogonal filterbanks by requiring all these angles to be close to  $90^\circ$ , where the angle between a vector  $\{h_k\}_{k \in \mathbb{Z}}$  and its even-integer shift  $\{h_{k+2\ell}\}_{k \in \mathbb{Z}}$  was conventionally defined and calculated by

$$\arccos \frac{\langle \{h_k\}_{k \in \mathbb{Z}}, \{h_{k+2\ell}\}_{k \in \mathbb{Z}} \rangle}{\|\{h_k\}_{k \in \mathbb{Z}}\|_2^2}, \quad \ell \in \mathbb{Z}. \quad (33)$$

The  $\mathbf{h}$  and  $\mathbf{g}$  had subsets of exactly equal coefficients, and lengths of both  $\mathbf{h}$  and  $\mathbf{g}$  were *even* only. Observe that all angles in (33) for  $\ell \in \mathbb{Z} \setminus \{0\}$  are close to  $90^\circ$  is equivalent to that all coefficients of  $z^\ell$  in  $|H(z)|^2 + |H(-z)|^2$  for  $\ell \in \mathbb{Z} \setminus \{0\}$  are close to zero, i.e.,  $\phi$  is near orthogonal.

A family  $\{f_k\}_{k \in \mathbb{Z}}$  of functions in a Hilbert space is a *Riesz basis*, if there are constants  $A, B > 0$  such that

$$A \|\{c_k\}_{k \in \mathbb{Z}}\|_2^2 \leq \left\| \sum_{k \in \mathbb{Z}} c_k f_k \right\|_2^2 \leq B \|\{c_k\}_{k \in \mathbb{Z}}\|_2^2, \quad (34)$$

for all  $\{c_k\}_{k \in \mathbb{Z}} \in \ell_2(\mathbb{R})$ , where  $A$  and  $B$  are the *lower Riesz bound* (LRB) and *upper Riesz bound* (URB) for  $\{f_k\}_{k \in \mathbb{Z}}$ . Saint-Martin et al. (de Saint-Martin et al., 1999) also concerned energy preserving and established two *even*-length biorthogonal filterbanks 26/14 and 18/10. The ratios of the upper and lower Riesz bounds were required to be close to one so the resulting biorthogonal filterbanks were nearly orthogonal, where the Riesz bounds were calculated iteratively. For the BFB 26/14 in (de Saint-Martin et al., 1999),  $w_{0,0} = .9951120811543$  and  $w_{0,1} = 1.0076522344272$ ; for the BFB 18/10 in (de Saint-Martin et al., 1999),  $w_{0,0} = 1.0210046900565$  and  $w_{0,1} = .9834108802518$ , so that they both preserved energy well, but the corresponding wavelets have only one vanishing moment.

We end this section by indicating that Appendix I gives a detailed procedure of how to evaluate both the LRB and the URB for refinable functions  $\phi$  and  $\tilde{\phi}$ . All LRB and URB of  $\phi$  and  $\tilde{\phi}$  for our new BFBs with certain EP conditions will be listed at the end of Section 5.

### 3. Weights in Terms of Two-Scale Sequences

On one hand, lowpass and highpass filters  $\{h_k\}_{k \in \mathbb{Z}}$  and  $\{g_k\}_{k \in \mathbb{Z}}$  derived from any orthonormal wavelet system  $(\phi, \psi)$  are *self-dual*. The filterbanks satisfy the Condition EP at any level of

decomposition, mainly due to the fact that

$$\sum_{k \in \mathbb{Z}} |h_k|^2 = \sum_{k \in \mathbb{Z}} |g_k|^2 = 1,$$

and the Rayleigh Energy Theorem or Parseval's Theorem

$$\|x\|^2 = \|X\|^2 = \int_{-\pi}^{\pi} |X(e^{-j\omega})|^2 d\omega,$$

where  $X$  is the normalized discrete Fourier transform of a discrete time sequence  $x$  with finite  $\ell_2$ -norm.

On the other hand, the energy of a biorthogonal wavelet system is not 100% preserved. Here, energy can be expressed in terms of the wavelet coefficients and can also be formulated by the variance of a signal's reconstructed output through its subband synthesis system. This variance, in turn, can be expressed in terms of the *weights*, or  $\ell_2$ -norm squares, of the lowpass and highpass filters (Woods and Naveen, 1992; Usevitch, 2001).

More precisely, let  $(\{h_k\}_{k \in \mathbb{Z}}, \{g_k\}_{k \in \mathbb{Z}})$  be the lowpass and highpass filters corresponding to a pair of refinable function and wavelet  $(\phi, \psi)$ . Introduce  $(\mathbf{h}_{\ell,0}, \mathbf{g}_{\ell,1})$ , with  $\ell \in \mathbb{Z}_+$  indicating the decomposition level, 0 for lowpass subband, and 1 for highpass subband, by

$$\mathbf{h}_{\ell,0} = \mathbf{h}_{\ell-1,0} * \{h_{2^\ell k}\}_{k \in \mathbb{Z}}, \quad (35)$$

$$\mathbf{g}_{\ell,1} = \mathbf{h}_{\ell-1,0} * \{g_{2^\ell k}\}_{k \in \mathbb{Z}}, \quad \ell = 1, 2, \dots, \quad (36)$$

$$\mathbf{h}_{0,0} = \{h_k\}_{k \in \mathbb{Z}}, \quad (37)$$

$$\mathbf{g}_{0,1} = \{g_k\}_{k \in \mathbb{Z}}, \quad (38)$$

where  $*$  indicates the usual convolution, and  $\{h_{2^\ell k}\}_{k \in \mathbb{Z}}$  and  $\{g_{2^\ell k}\}_{k \in \mathbb{Z}}$  are the  $\ell$ -th 2-upsampling of  $\{h_k\}_{k \in \mathbb{Z}}$  and  $\{g_k\}_{k \in \mathbb{Z}}$ . We define *weights* with respect to  $(\mathbf{h}, \mathbf{k}) = (\{h_k\}_{k \in \mathbb{Z}}, \{g_k\}_{k \in \mathbb{Z}})$ , by

$$w_{\ell,0} = \|\mathbf{h}_{\ell,0}\|^2, \quad (39)$$

$$w_{\ell,1} = \|\mathbf{g}_{\ell,1}\|^2, \quad \ell = 0, 1, 2, \dots \quad (40)$$

Similarly, let  $(\tilde{\mathbf{h}}, \tilde{\mathbf{k}}) = (\{\tilde{h}_k\}_{k \in \mathbb{Z}}, \{\tilde{g}_k\}_{k \in \mathbb{Z}})$  be the lowpass and highpass filters with respect to  $(\tilde{\phi}, \tilde{\psi})$  that is biorthogonal to  $(\phi, \psi)$ ; introduce  $(\tilde{\mathbf{h}}_{\ell,0}, \tilde{\mathbf{g}}_{\ell,1})$ ,  $\ell \in \mathbb{Z}_+$ , by

$$\tilde{\mathbf{h}}_{\ell,0} = \tilde{\mathbf{h}}_{\ell-1,0} * \{\tilde{h}_{2^\ell k}\}_{k \in \mathbb{Z}}, \quad (41)$$

$$\tilde{\mathbf{g}}_{\ell,1} = \tilde{\mathbf{h}}_{\ell-1,0} * \{\tilde{g}_{2^\ell k}\}_{k \in \mathbb{Z}}, \quad \ell = 1, 2, \dots, \quad (42)$$

$$\tilde{\mathbf{h}}_{0,0} = \{\tilde{h}_k\}_{k \in \mathbb{Z}}, \quad (43)$$

$$\tilde{\mathbf{g}}_{0,1} = \{\tilde{g}_k\}_{k \in \mathbb{Z}}; \quad (44)$$

and define *weights* with respect to  $(\tilde{\mathbf{h}}, \tilde{\mathbf{k}})$  by

$$\tilde{w}_{\ell,0} = \|\tilde{\mathbf{h}}_{\ell,0}\|^2, \quad (45)$$

$$\tilde{w}_{\ell,1} = \|\tilde{\mathbf{g}}_{\ell,1}\|^2, \quad \ell = 0, 1, 2, \dots \quad (46)$$

Conditions EP1–EP4 in (1)–(4) include specific criteria regarding how close is to one for each of these weights at the initial level. For instance, Condition EP1 means minimizing  $w_{0,1} - 1$  under the condition  $w_{0,0} = 1$ .

We end this section by pointing out the following.

*Proposition 1:* The weights in (39)–(40) can also be determined by the constant term of the two-scale symbols  $H$  and  $G$  of  $\phi$  and  $\psi$ , i.e.,

$$w_{\ell,0} = \text{the constant term of } 2^{\ell+1} \prod_{k=0}^{\ell} \left| H(z^{2^k}) \right|^2, \quad (47)$$

$$w_{\ell,1} = \text{the constant term of } 2^{\ell+1} \left| G(z^{2^\ell}) \right|^2 \prod_{k=0}^{\ell-1} \left| H(z^{2^k}) \right|^2, \quad (48)$$

for  $\ell = 0, 1, 2, \dots$

**Proof.** A straightforward application of the fact that the  $z$ -transform of a convolution of two sequences is the product of their  $z$ -transforms provides proof of Proposition 1. In details, without loss of generality, represent the  $z$ -transform of a sequence  $\{a_k\}_{k \in \mathbb{Z}}$  by

$$\mathcal{Z}[\{a_k\}_{k \in \mathbb{Z}}](z) = \sum_{k \in \mathbb{Z}} a_k z^{-k}.$$

Then, take the  $z$ -transforms of (35) both sides to obtain

$$\begin{aligned} \mathcal{Z}[\mathbf{h}_{\ell,0}](z) &= \mathcal{Z}[\mathbf{h}_{\ell-1,0}](z) \mathcal{Z}[\{h_{2^\ell k}\}_{k \in \mathbb{Z}}](z) \\ &= \mathcal{Z}[\mathbf{h}_{\ell-1,0}](z) \sqrt{2} H(z^{-2^\ell}) \\ &= \mathcal{Z}[\mathbf{h}_{0,0}](z) (\sqrt{2})^\ell \prod_{k=1}^{\ell} H(z^{-2^k}) \\ &= (\sqrt{2})^{\ell+1} \prod_{k=0}^{\ell} H(z^{-2^k}), \end{aligned}$$

where  $H$  in (8) has been used in the second equality. Similarly, utilize this result and  $G$  in (10) and take the  $z$ -transforms of (36) both sides to yield

$$\begin{aligned} \mathcal{Z}[\mathbf{g}_{\ell,1}](z) &= \mathcal{Z}[\mathbf{h}_{\ell-1,0}](z) \mathcal{Z}[\{g_{2^\ell k}\}_{k \in \mathbb{Z}}](z) \\ &= (\sqrt{2})^{\ell+1} G(z^{-2^\ell}) \prod_{k=0}^{\ell-1} H(z^{-2^k}). \end{aligned}$$

The conclusion follows simply by using the fact that

$$\sum_{k \in \mathbb{Z}} |a_k|^2 = \text{the constant term of } \left( \sum_{k \in \mathbb{Z}} a_k z^k \right) \left( \sum_{k \in \mathbb{Z}} a_k z^{-k} \right).$$

This completes the proof of Proposition 1.



#### 4. An Algorithm for Constructing Biorthogonal Refinable Functions and Wavelets

Let  $(\phi, \psi)$  and  $(\tilde{\phi}, \tilde{\psi})$  be a biorthogonal pair of refinable functions and wavelets, with two-scale symbols  $(H, G)$  and  $(\tilde{H}, \tilde{G})$ . For both  $\phi$  and  $\tilde{\phi}$  to have even-length supports and both  $\psi$  and  $\tilde{\psi}$  to have  $2m$  vanishing moments (VM),  $H$  and  $\tilde{H}$  can be written as

$$H(z) = \left(\frac{1+z}{2}\right)^{2m} S_{2n}(z), \quad (49)$$

$$\tilde{H}(z) = z \left(\frac{1+z}{2}\right)^{2m} \tilde{S}_{2n-2}(z), \quad (50)$$

where both  $S_{2n}$  and  $\tilde{S}_{2n-2}$  are reciprocal polynomials of exact degrees  $2n$  and  $2n-2$ , and satisfy

$$(1+z) \nmid S_{2n}(z), \quad (1+z) \nmid \tilde{S}_{2n-2}(z);$$

$$S_{2n}(1) = \tilde{S}_{2n-2}(1) = 1.$$

Here, a (Laurent) polynomial is *reciprocal* if it is symmetric, e.g.,  $P(z) = -3/z + 2 + z + 2z^2 - 3z^3$  is reciprocal since  $P(1/z) = z^2 P(z)$ . By doing so, the filterbanks will be CDF  $(2m+2n+1)/(2m+2n-1)$ , i.e., both lowpass and highpass filters are with linear phases and both have odd lengths. The integer  $K$  in (12) or (18)–(19) is  $K = m+n$ . By selecting  $\varepsilon = (-1)^{m+n+1}$  (so that both  $\psi$  and  $\tilde{\psi}$  look better in graphs),  $G$  and  $\tilde{G}$  in (18) and (19) can simply be calculated by

$$G(z) = (-1)^{m+n} z^{-1} \tilde{H}(-z), \quad (51)$$

$$\tilde{G}(z) = (-1)^{m+n} z^{-1} H(-z). \quad (52)$$

As immediate simple examples, the LeGall 5/3 is when  $m = n = 1$ , while the CDF 9/7 is when  $m = n = 2$ .

With the introduction of

$$t = \frac{1}{2} \left(1 - \frac{z^{-1} + z}{2}\right), \quad (53)$$

the two polynomials  $H$  and  $\tilde{H}$  in (49)–(50) can also be expressed as

$$H(z) = z^{m+n} (1-t)^m F_n(t), \quad (54)$$

$$\tilde{H}(z) = z^{m+n} (1-t)^m G_{n-1}(t), \quad (55)$$

for some polynomials  $F_n$  and  $G_{n-1}$  of exact degrees  $n$  and  $n-1$  that satisfy

$$F_n(0) = G_{n-1}(0) = 1. \quad (56)$$

The identity (20) then becomes

$$(1-t)^{2m} F_n(t) G_{n-1}(t) + t^{2m} F_n(1-t) G_{n-1}(1-t) = 1, \quad t \in [0, 1]. \quad (57)$$

Observe that  $n \geq m$  in order for (57) to have any solution. Hence, it then follows from (Lian, 2001) that  $F_n G_{n-1}$  must have the form

$$F_n(t)G_{n-1}(t) = \sum_{k=0}^{2m-1} \binom{2m-1+k}{k} t^k + t^{2m}(1-2t)f_{n-m-1}((1-2t)^2), \quad (58)$$

where  $f_{n-m-1}$  is a polynomial of exact degree  $n-m-1$ .

In summary, here is an algorithm for constructing biorthogonal refinable functions and wavelets, and consequently their corresponding BFBs.

**Algorithm 1 (for Constructing BFB with Condition EP): Step 1.**

- (1) For  $\psi$  and  $\tilde{\psi}$  to have  $2m$  vanishing moments, select an integer  $n > m$ ; and write explicitly the three polynomials  $F_n$ ,  $G_{n-1}$ , and  $f_{n-m-1}$  of exact degrees  $n$ ,  $n-1$ , and  $n-m-1$ , respectively.
- (2) The identity (58), with the condition (56), gives rise to  $2n-1$  equalities for the  $n$ ,  $n-1$ , and  $n-m$  to-be-determined coefficients in  $F_n$ ,  $G_{n-1}$ , and  $f_{n-m-1}$ . (Although the  $2n-1$  equations constitute a nonlinear system, there should still be  $n-m$  additional freedoms.)
- (3) For Condition EP1, minimize  $w_{0,1} - 1$  under the condition  $w_{0,0} = 1$ ; for Condition EP2, minimize  $w_{0,0} - 1$  under the condition  $w_{0,1} = 1$ ; for Condition EP3, minimize  $w_{0,0} - 1$  (or  $w_{0,1} - 1$ ) under the condition  $w_{0,0} = w_{0,1}$ ; for Condition EP4, minimize  $(w_{0,0} - 1)^2 + (w_{0,1} - 1)^2$ .
- (4) After both  $F_n$  and  $G_{n-1}$  being fixed, both  $H$  and  $\tilde{H}$  are determined by (54)–(55), with  $t$  in (53); and  $G$  and  $\tilde{G}$  are determined from  $H$  and  $\tilde{H}$  through (51)–(52).
- (5) With  $H$ ,  $G$ ,  $\tilde{H}$ , and  $\tilde{G}$  being determined, BFB  $(2m+2n+1)/(2m+2n-1)$  filters with appropriate EP conditions are consequently established through (8), (10), (14), and (16).

As convenient examples, for LeGall 5/3,  $m = n = 1$  and

$$F_1(t) = 1 + 2t, \quad G_0(t) = 1;$$

for CDF 9/7,  $m = n = 2$  and

$$F_2(t)G_1(t) = 1 + 4t + 10t^2 + 20t^3,$$

which leads to

$$F_2(t) = 1 + a_1 t + a_2 t^2, \quad (59)$$

$$G_1(t) = 1 + b_1 t, \quad (60)$$

where the three coefficients  $a_1$ ,  $a_2$ , and  $b_1$  in (59)–(60) are explicitly expressed by

$$a_1 = \frac{8}{3} - \frac{1}{3}\alpha + \frac{3\sqrt{15} - 11}{42}\alpha^2, \quad (61)$$

$$a_2 = \frac{10}{3} - \frac{5 - \sqrt{15}}{3}\alpha + \frac{2\sqrt{15} - 5}{21}\alpha^2, \quad (62)$$

$$b_1 = \frac{4}{3} + \frac{1}{3}\alpha - \frac{3\sqrt{15} - 11}{42}\alpha^2, \quad (63)$$

with  $\alpha$  already having been introduced in (28). For comparison purposes, weights for LeGall 5/3 are calculated and listed in Table 1. It is clear that they do not satisfy any of the four EP conditions in (1)–(4); and the weights are relatively away from 1. Weights for CDF 9/7 are also calculated by using our formulations in (35)–(40) and (41)–(46), and included in Table 2. Though CDF 9/7 does not satisfy any of the four EP conditions in (1)–(4), Table 2 clearly indicates that CDF 9/7 filters do preserve energy for all the first 4 levels very well (as all weights are relatively close to 1).

We end this section by mentioning that the scenario  $n = m$  in Algorithm 1 corresponds to the CDF  $(4m + 1)/(4m - 1)$  in the literature (of both wavelets and image and signal processing). By allowing  $n \geq m + 1$ , we have more flexibility or can require  $H$  and  $\tilde{H}$  to satisfy certain desirable conditions, such as our newly proposed EP conditions.

Table 1. Weights of LeGall 5/3, with  $\mathbf{h} = \frac{1}{\sqrt{2}} \left\{ -\frac{1}{4}, \frac{1}{2}, \frac{3}{2}, \frac{1}{2}, -\frac{1}{4} \right\}$  and  $\tilde{\mathbf{h}} = \frac{1}{\sqrt{2}} \left\{ \frac{1}{2}, 1, \frac{1}{2} \right\}$

Weights	$\mathbf{h}$	$\tilde{\mathbf{h}}$	Weights
$w_{0,0}$	1.4375000000000000	.7500000000000000	$\tilde{w}_{0,0}$
$w_{0,1}$	.7500000000000000	1.4375000000000000	$\tilde{w}_{0,1}$
$w_{1,0}$	1.7382812500000000	.6875000000000000	$\tilde{w}_{1,0}$
$w_{1,1}$	1.3359375000000000	.9218750000000000	$\tilde{w}_{1,1}$
$w_{2,0}$	1.9162597656250000	.6718750000000000	$\tilde{w}_{2,0}$
$w_{2,1}$	1.7592773437500000	.7929687500000000	$\tilde{w}_{2,1}$
$w_{3,0}$	2.0167999267578125	.6679687500000000	$\tilde{w}_{3,0}$
$w_{3,1}$	2.0131530761718750	.7607421875000000	$\tilde{w}_{3,1}$

Table 2. Weights of CDF 9/7

Weights	$\mathbf{h}$	$\tilde{\mathbf{h}}$	Weights
$w_{0,0}$	1.0404359637949253	.9829536572876483	$\tilde{w}_{0,0}$
$w_{0,1}$	.9829536572876483	1.0404359637949253	$\tilde{w}_{0,1}$
$w_{1,0}$	.9938066630262757	1.0306024684922561	$\tilde{w}_{1,0}$
$w_{1,1}$	1.1186419424407187	.9672158060329819	$\tilde{w}_{1,1}$
$w_{2,0}$	.9708630123538691	1.0520930222440912	$\tilde{w}_{2,0}$
$w_{2,1}$	1.0443177567099245	1.0396277874758167	$\tilde{w}_{2,1}$
$w_{3,0}$	.9633462544497677	1.0584732545638578	$\tilde{w}_{3,0}$
$w_{3,1}$	1.0037017315870575	1.0751205695491978	$\tilde{w}_{3,1}$

## 5. New BFBs with Appropriate EP Conditions

We utilize the efficient Algorithm 1 in Section 4 to build a new family of compactly supported biorthogonal refinable functions and wavelets, such that their corresponding BFBs satisfy one of the four EP conditions in (1)–(4). The selected values for  $m$  in (49)–(50) will be 1, 2, and 3, so that the numbers of VM for the corresponding wavelets will be 2, 4, and 6.

### 5.1. BFB 7/5 with Condition EP4: $m = 1$ and $n = 2$ .

By writing the two polynomials  $F_2$  and  $G_1$  in (54)–(55) explicitly as

$$F_2(t) = 1 + a_1t + a_2t^2, \quad (64)$$

$$G_1(t) = 1 + b_1t, \quad (65)$$

it follows from (58) that they must satisfy

$$F_2(t)G_1(t) = 1 + 2t + C_0t^2(1 - 2t), \quad (66)$$

for some constant  $C_0$ . Solve (64)–(66) for  $a_1$ ,  $a_2$ , and  $C_0$  to obtain

$$a_1 = 2 - b_1, \quad a_2 = \frac{2b_1(b_1 - 2)}{b_1 + 2}, \quad C_0 = -\frac{b_1^2(b_1 - 2)}{b_1 + 2}, \quad (67)$$

with the last parameter  $b_1$  to be determined from one of the four EP conditions. For instance,  $w_{0,0} = \|\mathbf{h}\|_2^2 = 1$  in Condition EP1 leads to

$$b_1^4 - 12b_1^3 - 68b_1^2 - 192b_1 + 224 = 0, \quad (68)$$

while  $w_{0,1} = \|\mathbf{g}\|_2^2$  in Condition EP1 will remain a constant close to 1. Similarly, with Condition EP2, Condition EP3, and Condition EP4,  $b_1$  is governed by

$$3b_1^2 + 16b_1 - 16 = 0, \quad (69)$$

$$5b_1^4 + 68b_1^3 + 188b_1^2 + 192b_1 - 352 = 0, \quad (70)$$

$$\begin{aligned} 37b_1^8 + 634b_1^7 + 4560b_1^6 + 17424b_1^5 + 36720b_1^4 \\ + 43488b_1^3 + 21760b_1^2 + 40192b_1 - 109588 = 0, \end{aligned} \quad (71)$$

respectively. Solving (68)–(71) numerically, solutions for  $b_1$  satisfying Condition EP1–Condition EP4 are given by

$$b_1 = .8645028006282423, \quad (72)$$

$$b_1 = .8610017480861208, \quad (73)$$

$$b_1 = .8627181302055645, \quad (74)$$

$$b_1 = .8626844958636667. \quad (75)$$

We point out that the value  $b_1$  in (73) was also obtained in (Cohen et al., 1992) and (Daubechies, 1992, p.283) where the expression in (29) was minimized, or equivalently,  $w_{0,0} = 1$ . Similar

BFBs were also constructed in (Antonini et al., 1992), where filter entries were rational numbers, namely,

$$\{h_k\}_{k=-3,\dots,3} = \frac{1}{280\sqrt{2}} \{-3, -15, 73, 170, 73, -15, -3\},$$

$$\{\tilde{h}_k\}_{k=-2,\dots,2} = \frac{1}{20\sqrt{2}} \{-1, 5, 12, 5, -1\}.$$

Here, by using our notations, the corresponding  $b_1$  in (65), and consequently  $a_1$ ,  $a_2$ , and  $C_0$  in (67) are

$$b_1 = \frac{4}{5}; \quad a_1 = \frac{6}{5}, \quad a_2 = -\frac{24}{35}; \quad C_0 = \frac{48}{175};$$

and the weights  $w_{0,0}$  and  $w_{0,1}$  in (45)–(46) are

$$w_{0,0} = \frac{2859}{2800} = 1.0210714285714286,$$

$$w_{0,1} = \frac{49}{50} = .98.$$

Turning to the four values for  $b_1$  in (72)–(75), they are all close to each other. We here only focus on the BFB with Condition EP4 in this section, i.e., with  $b_1$  in (75). We use  $\phi_{7,5}^{EP4}$ ,  $\psi_{7,5}^{EP4}$ ,  $\tilde{\phi}_{7,5}^{EP4}$ , and  $\tilde{\psi}_{7,5}^{EP4}$  to denote the corresponding biorthogonal refinable functions and wavelets. It follows from (54)–(55), (64)–(65), (67), and (75), the BFB 7/5 with Condition EP4 is created and listed in Table 3.

Table 3. BFB 7/5 with Condition EP4

$k$	$\mathbf{h}$	$\mathbf{g}$	$k$
0, 6	-.0151469253895285	-.0762512571312121	0, 4
1, 5	-.0702315873863679	-.3535533905932738	1, 3
2, 4	.3687003159828022	.8596092954489717	2
3	.8475699559592833		
$k$	$\mathbf{h}$	$\tilde{\mathbf{g}}$	$k$
1, 5	-.0762512571312121	.0151469253895285	-1, 5
2, 4	.3535533905932738	-.0702315873863679	0, 4
3	.8596092954489717	-.3687003159828022	1, 3
		.8475699559592833	2

Weights of the BFB 7/5 with Condition EP4 are illustrated in Table 4. The graphs of  $\phi_{7,5}^{EP4}$ ,  $\psi_{7,5}^{EP4}$ ,  $\tilde{\phi}_{7,5}^{EP4}$ , and  $\tilde{\psi}_{7,5}^{EP4}$  are plotted in Fig. 1. Additional three BFB 7/5's with Conditions EP1–EP3 are included in the Appendix II.

## 5.2. BFB 9/7 with Condition EP1: $m = 1$ and $n = 3$ .

Using  $\phi_{9,7}^{EP1}$ ,  $\psi_{9,7}^{EP1}$ ,  $\tilde{\phi}_{9,7}^{EP1}$ , and  $\tilde{\psi}_{9,7}^{EP1}$  to denote the biorthogonal refinable functions and wavelets, it follows from (56)–(58) that we need to find  $F_3$  and  $G_2$ , e.g.,

$$F_3(t) = 1 + a_1 t + a_2 t^2 + a_3 t^3, \quad (76)$$

$$G_2(t) = 1 + b_1 t + b_2 t^2, \quad (77)$$

Table 4. Weights of BFB 7/5 with Condition EP4

Weights	$\mathbf{h}$	$\tilde{\mathbf{h}}$	Weights
$w_{0,0}$	1.0005784866875877	1.0005566492504580	$\tilde{w}_{0,0}$
$w_{0,1}$	1.0005566492504580	1.0005784866875877	$\tilde{w}_{0,1}$
$w_{1,0}$	1.0076302279709638	.9942931852525390	$\tilde{w}_{1,0}$
$w_{1,1}$	.9949013664034054	1.0082125289423012	$\tilde{w}_{1,1}$
$w_{2,0}$	1.0109731444897238	.9911227078550452	$\tilde{w}_{2,0}$
$w_{2,1}$	1.0055307248134918	.9987303196390679	$\tilde{w}_{2,1}$
$w_{3,0}$	1.0121574495762324	.9898977949364849	$\tilde{w}_{3,0}$
$w_{3,1}$	1.0109555946963996	.9935355807715416	$\tilde{w}_{3,1}$

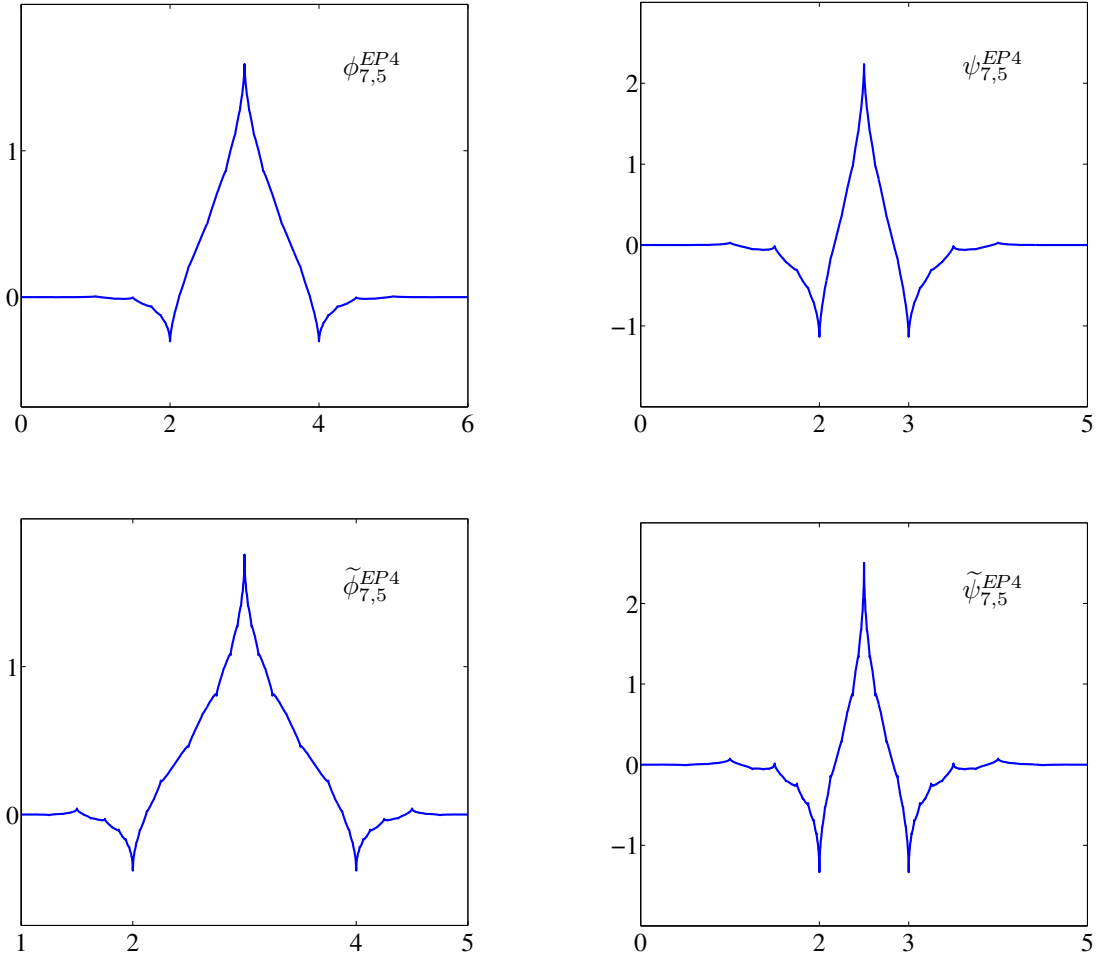


Figure 1. Plots of refinable functions and wavelets for BFB 7/5 with Condition EP4:  $\phi_{7,5}^{EP4}$ ,  $\psi_{7,5}^{EP4}$ ,  $\tilde{\phi}_{7,5}^{EP4}$ , and  $\tilde{\psi}_{7,5}^{EP4}$ .

so that they satisfy

$$F_3(t)G_2(t) = 1 + 2t + t^2(1 - 2t)(C_0 + C_1(1 - 2t)^2), \quad (78)$$

for some constants  $C_0$  and  $C_1$ .

We focus on BFB filters, derived from the refinable function  $\phi$  and wavelet  $\psi$ , satisfying Condition EP1 in (1), i.e.,

$$w_{0,0} = 1, \quad |w_{0,1} - 1| = \text{the smallest.} \quad (79)$$

To demonstrate the elegance of our Algorithm 1, we enumerate the procedure for calculating the 7 to-be-determined coefficients  $a_1, a_2, a_3, b_1, b_2, C_0$ , and  $C_1$  in details (similar details will be omitted for the remaining seven constructions in the sequel).

First of all, the identity (78) yields 5 equations involving the 7 coefficients  $a_1, a_2, a_3, b_1, b_2, C_0$ , and  $C_1$ , namely,

$$a_1 + b_1 - 2 = 0, \quad (80)$$

$$a_2 + a_1b_1 + b_2 - C_0 - C_1 = 0, \quad (81)$$

$$a_1b_2 + a_2b_1 + a_3 + 2C_0 + 6C_1 = 0, \quad (82)$$

$$a_2b_2 + a_3b_1 - 12C_1 = 0, \quad (83)$$

$$a_3b_2 + 8C_1 = 0. \quad (84)$$

Solve the 5 equations (80)–(84) in such a way that  $a_1, a_2, a_3, C_0$  and  $C_1$  are being expressed in terms of  $b_1$  and  $b_2$ :

$$a_1 = -b_1 + 2, \quad (85)$$

$$a_2 = \frac{(2b_1 + 3b_2)(b_1b_2 + 2b_1^2 - 4b_1 - 4b_2)}{(b_1 + b_2)(2b_1 + b_2 + 4)}, \quad (86)$$

$$a_3 = -\frac{2b_2(b_2b_1 - 4b_2 + 2b_1^2 - 4b_1)}{(b_1 + b_2)(2b_1 + b_2 + 4)}, \quad (87)$$

$$C_0 = -\frac{1}{4}(b_2^3b_1 - 8b_2^3 + 6b_2^2b_1^2 - 36b_2^2b_1 - 48b_2b_1^2 + 32b_2b_1 - 16b_1^3 + 32b_2^2 + 8b_1^4 + 12b_1^3b_2)/((b_1 + b_2)(2b_1 + b_2 + 4)), \quad (88)$$

$$C_1 = \frac{1}{4} \frac{b_2^2(b_2b_1 - 4b_2 + 2b_1^2 - 4b_1)}{(b_1 + b_2)(2b_1 + b_2 + 4)}. \quad (89)$$

Second, by using (53)–(55) and (18), the two conditions in (79) are

$$w_{0,0} = \text{the constant term of } 2(1-t)^2 F_3(t)^2 \Big|_{t=\frac{1}{2}(1-\frac{z^{-1}+z}{2})} = 1, \quad (90)$$

and

$$w_{0,1} - 1 = \text{the constant term of } 2(1-t)^2 G_2(t)^2 \Big|_{t=\frac{1}{2}(1-\frac{z^{-1}+z}{2})} - 1 = \text{the smallest.} \quad (91)$$

With (85)–(89), the requirement (90) leads to

$$\begin{aligned} & 28672b_2^2 + 28672b_1^2 + 57344b_2b_1 - 58368b_2b_1^2 - 43008b_2^2b_1 - 9216b_2^3 - 10144b_2^3b_1 \\ & - 25168b_2^2b_1^2 - 25088b_1^3b_2 - 1736b_2^3b_1^2 - 4016b_2^2b_1^3 - 4096b_2b_1^4 - 24576b_1^3 \\ & - 8704b_1^4 - 1360b_2^4 - 1536b_1^5 + 128b_1^6 - 280b_2^4b_1 + 11b_2^4b_1^2 \\ & + 76b_2^3b_1^3 + 204b_2^2b_1^4 + 256b_2b_1^5 = 0, \end{aligned} \quad (92)$$

while, by denoting  $w_{0,1} - 1$  in (91) by  $T(b_1, b_2)$ , meaning the *target* function,  $T(b_1, b_2)$  becomes

$$T(b_1, b_2) = \frac{1}{512}(24b_1^2 + 24b_1b_2 + 7b_2^2 + 128b_1 + 48b_2 - 128). \quad (93)$$

Third, a direct application of the method of Lagrange multipliers to finding local extrema of the target function  $T(b_1, b_2)$  in (93) under the constraint (92) gives rise to a group of four solutions for  $b_1$  and  $b_2$ . The best solution among these four solutions that minimizes  $T(b_1, b_2)$  in (93) is

$$b_1 = 1.0165426408592217, \quad b_2 = -.3862070404605876,$$

so that

$$\begin{aligned} a_1 &= .9834573591407783, & a_2 &= -.2081412616407905, \\ a_3 &= -.1838511497717023, & C_0 &= .4142536149868504, \\ C_1 &= -.0088755760548257. \end{aligned}$$

Finally, with these seven coefficients and by using (53)–(55) and (51)–(52), all linear-phase filters for the BFB 9/7 with Condition EP1 are established and listed in Table 5.

Weights of the BFB 9/7 with Condition EP1 are illustrated in Table 6, and graphs of  $\phi_{9,7}^{EP1}$ ,  $\psi_{9,7}^{EP1}$ ,  $\tilde{\phi}_{9,7}^{EP1}$ , and  $\tilde{\psi}_{9,7}^{EP1}$  are plotted in Fig. 2.

Table 5. BFB 9/7 with Condition EP1

$k$	$\mathbf{h}$	$\mathbf{g}$	$k$
0, 8	.0010156437088478	.0085340505391147	0, 6
1, 7	-.0086618903838575	-.0727824232613753	1, 5
2, 6	-.0736649650247083	-.3620874411323884	2, 4
3, 5	.3622152809771313	.8526716277092981	3
4	.8524054238182686		
$k$	$\tilde{\mathbf{h}}$	$\tilde{\mathbf{g}}$	$k$
1, 7	-.0085340505391147	.0010156437088478	-1, 7
2, 6	-.0727824232613753	.0086618903838575	0, 6
3, 5	.3620874411323884	-.0736649650247083	1, 5
4	.8526716277092981	-.3622152809771313	2, 4
		.8524054238182686	3

Table 6. Weights of BFB 9/7 with Condition EP1

Weights	$\mathbf{h}$	$\tilde{\mathbf{h}}$	Weights
$w_{0,0}$	1.0000000000000000	1.0000037570608299	$\tilde{w}_{0,0}$
$w_{0,1}$	1.0000037570608299	1.0000000000000000	$\tilde{w}_{0,1}$
$w_{1,0}$	0.9990932489588953	1.0009111516155897	$\tilde{w}_{1,0}$
$w_{1,1}$	1.0009115240449724	.9991011381205513	$\tilde{w}_{1,1}$
$w_{2,0}$	.9986816393628597	1.0013234581092678	$\tilde{w}_{2,0}$
$w_{2,1}$	.9995090864790113	1.0005030836707783	$\tilde{w}_{2,1}$
$w_{3,0}$	.9985328256234965	1.0014729408738587	$\tilde{w}_{3,0}$
$w_{3,1}$	.9988343927834451	1.0011779289611062	$\tilde{w}_{3,1}$



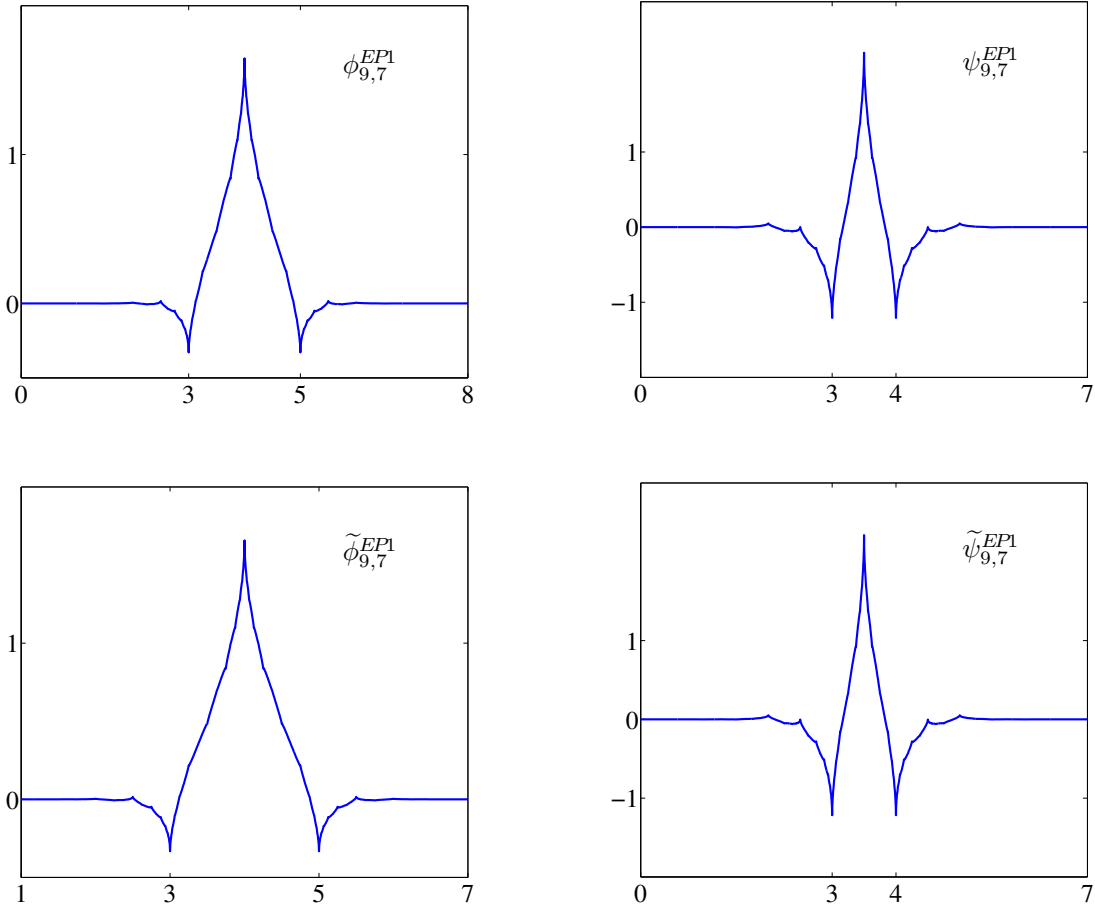


Figure 2. Plots of refinable functions and wavelets for BFB 9/7 with Condition EP1:  $\phi_{9,7}^{EP1}$ ,  $\psi_{9,7}^{EP1}$ ,  $\tilde{\phi}_{9,7}^{EP1}$ , and  $\tilde{\psi}_{9,7}^{EP1}$ .

### 5.3. BFB 9/7 with Condition EP2: $m = 1$ and $n = 3$ .

The biorthogonal refinable functions and wavelets are denoted by  $\phi_{9,7}^{EP2}$ ,  $\psi_{9,7}^{EP2}$ ,  $\tilde{\phi}_{9,7}^{EP2}$ , and  $\tilde{\psi}_{9,7}^{EP2}$ . Completely analogous to the previous BFB 9/7, we simply change the two conditions for Condition EP1 in (79) to those for Condition EP2, namely,

$$w_{0,1} = 1, \quad |w_{0,0} - 1| = \text{the smallest.} \quad (94)$$

Exact procedure yields slightly different values for the coefficients of  $F_3$  and  $G_2$  in (76)–(77), as follows:

$$\begin{aligned} a_1 &= .9834776030341662, & a_2 &= -.2081618721169732, \\ a_3 &= -.1838536169545349, & b_1 &= 1.0165223969658338, \\ b_2 &= -.3861851306324918, & C_0 &= .4142551992841438, \\ C_1 &= -.0088751916351054, \end{aligned}$$

which consequently gives rise to the BFB in Table 7.

Table 7. BFB 9/7 with Condition EP2

$k$	$\mathbf{h}$	$\mathbf{g}$	$k$
0, 8	.0010156573382361	.0085335663957390	0, 6
1, 7	-.0086624003328945	-.0727816022238401	1, 5
2, 6	-.0736657889684743	-.3620869569890128	2, 4
3, 5	.3622157909261683	.8526699856342277	3
4	.8524070444470239		
$k$	$\tilde{\mathbf{h}}$	$\tilde{\mathbf{g}}$	$k$
1, 7	-.0085335663957390	.0010156573382361	-1, 7
2, 6	-.0727816022238401	.0086624003328945	0, 6
3, 5	.3620869569890128	-.0736657889684743	1, 5
4	.8526699856342277	-.3622157909261683	2, 4
		.8524070444470239	3

Weights of the BFB 9/7 with Condition EP2 are illustrated in Table 8, with graphs of  $\phi_{9,7}^{EP2}$ ,  $\psi_{9,7}^{EP2}$ ,  $\tilde{\phi}_{9,7}^{EP2}$ , and  $\tilde{\psi}_{9,7}^{EP2}$  plotted in Fig. 3.

Again, two additional BFB 9/7 with Condition EP3 and Condition EP4 are included in the Appendix II.

Table 8. Weights of BFB 9/7 with Condition EP2

Weights	$\mathbf{h}$	$\tilde{\mathbf{h}}$	Weights
$w_{0,0}$	1.0000037622228576	1.0000000000000000	$\tilde{w}_{0,0}$
$w_{0,1}$	1.0000000000000000	1.0000037622228576	$\tilde{w}_{0,1}$
$w_{1,0}$	.9990988954780349	1.0009054989309133	$\tilde{w}_{1,0}$
$w_{1,1}$	1.0009134049382975	.9990992796363417	$\tilde{w}_{1,1}$
$w_{2,0}$	.9986879784923395	1.0013171027585935	$\tilde{w}_{2,0}$
$w_{2,1}$	.9995140471602881	1.0004981404135577	$\tilde{w}_{2,1}$
$w_{3,0}$	.9985393907845092	1.0014663545786470	$\tilde{w}_{3,0}$
$w_{3,1}$	.9988405145018811	1.0011718131709768	$\tilde{w}_{3,1}$

#### 5.4. BFB 11/9 with Condition EP3: $m = 2$ and $n = 3$ .

The biorthogonal refinable functions and wavelets are denoted by  $\phi_{11,9}^{EP3}$ ,  $\psi_{11,9}^{EP3}$ ,  $\tilde{\phi}_{11,9}^{EP3}$ , and  $\tilde{\psi}_{11,9}^{EP3}$ . Again, write  $F_3$  and  $G_2$  the same as in (76)–(77). By using (56)–(58),  $F_3$  and  $G_2$  must satisfy

$$F_3(t)G_2(t) = 1 + 4t + 10t^2 + 20t^3 + C_0t^4(1 - 2t), \quad (95)$$

for some constant  $C_0$ . It turns out that, with (95) and the first condition of Condition EP3, all coefficients are settled. Among all possible solutions, select the one that satisfies the minimum  $\ell_2$ -norm in Condition EP3. By doing so, we arrive at

$$\begin{aligned} a_1 &= 1.0097370825100568, & a_2 &= 6.7709624774527519, \\ a_3 &= -.4586576392294149, & b_1 &= 2.9902629174899432, \\ b_2 &= .2096581683029422, & C_0 &= .0480806602594954, \end{aligned}$$

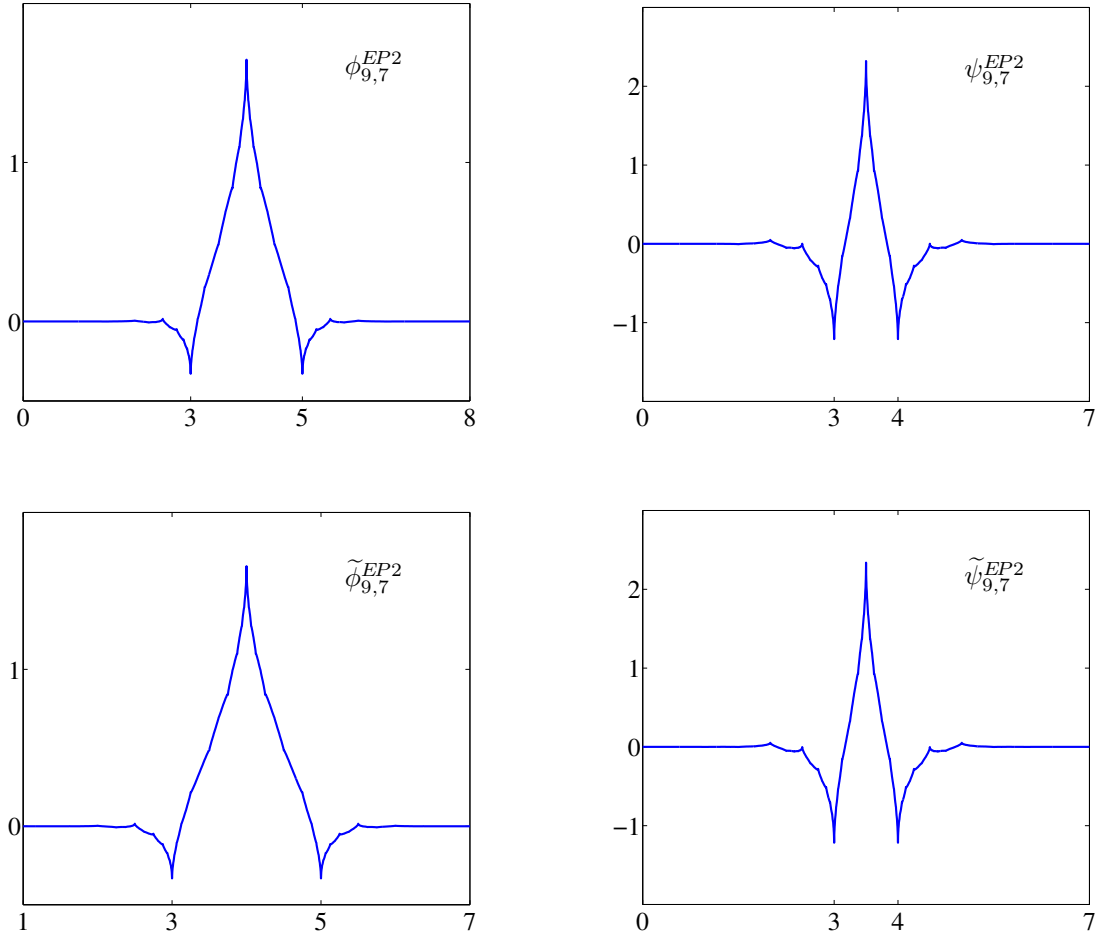


Figure 3. Plots of refinable functions and wavelets for BFB 9/7 with Condition EP2:  $\phi_{9,7}^{EP2}$ ,  $\psi_{9,7}^{EP2}$ ,  $\tilde{\phi}_{9,7}^{EP2}$ , and  $\tilde{\psi}_{9,7}^{EP2}$ .

which gives rise to the BFB in Table 9. Weights of the BFB 11/9 with Condition EP3 are illustrated in Table 10. Graphs of  $\phi_{11,9}^{EP3}$ ,  $\psi_{11,9}^{EP3}$ ,  $\tilde{\phi}_{11,9}^{EP3}$ , and  $\tilde{\psi}_{11,9}^{EP3}$  are plotted in Fig. 4. Once more, the other additional BFB 11/9 with Conditions EP4 only is provided in the Appendix II.

### 5.5. BFB 13/11 with Condition EP1: $m = 2$ and $n = 4$ .

The biorthogonal refinable functions and wavelets are denoted by  $\phi_{13,11}^{EP1}$ ,  $\psi_{13,11}^{EP1}$ ,  $\tilde{\phi}_{13,11}^{EP1}$ , and  $\tilde{\psi}_{13,11}^{EP1}$ . Similar to (76)–(77), write  $F_4$  and  $G_3$  as

$$F_4(t) = 1 + a_1t + a_2t^2 + a_3t^3 + a_4t^4, \quad (96)$$

$$G_3(t) = 1 + b_1t + b_2t^2 + b_3t^3. \quad (97)$$

The identity that  $F_4$  and  $G_3$  must satisfy, from (58), is

$$F_4(t)G_3(t) = 1 + 4t + 10t^2 + 20t^3 + t^4(1 - 2t)(C_0 + C_1(1 - 2t)^2), \quad (98)$$

Table 9. BFB 11/9 with Condition EP3

$k$	$\mathbf{h}$	$\mathbf{g}$	$k$
0, 10	.0006334373573089	.0011582086917044	0, 8
1, 9	.0361377618710581	.0660760995777440	1, 7
2, 8	-.0242125601425010	-.0483966862739871	2, 6
3, 7	-.1007871959770629	-.4196294901710178	3, 5
4, 6	.3771325133784659	.8015837363511130	4
5	.8364056493985571		
$k$	$\tilde{\mathbf{h}}$	$\tilde{\mathbf{g}}$	$k$
1, 9	.0011582086917044	-.0006334373573089	-1, 9
2, 8	.0660760995777440	.0361377618710581	0, 8
3, 7	-.0483966862739871	.0242125601425010	1, 7
4, 6	-.4196294901710178	-.1007871959770629	2, 6
5	.8015837363511130	-.3771325133784659	3, 5
		.8364056493985571	4

Table 10. Weights of BFB 11/9 with Condition EP3

Weights	$\mathbf{h}$	$\tilde{\mathbf{h}}$	Weights
$w_{0,0}$	1.0081335676751557	1.0081335676751557	$\tilde{w}_{0,0}$
$w_{0,1}$	1.0081335676751557	1.0081335676751557	$\tilde{w}_{0,1}$
$w_{1,0}$	.9541164667665928	1.0655080241114951	$\tilde{w}_{1,0}$
$w_{1,1}$	1.0852491451960252	.9745025929210217	$\tilde{w}_{1,1}$
$w_{2,0}$	.9302457372972378	1.0905114015916696	$\tilde{w}_{2,0}$
$w_{2,1}$	.9960085866006116	1.0610423509148224	$\tilde{w}_{2,1}$
$w_{3,0}$	.9227785728377510	1.0979194977962053	$\tilde{w}_{3,0}$
$w_{3,1}$	.9531638802345701	1.1017627855395372	$\tilde{w}_{3,1}$

where  $C_0$  and  $C_1$  are to-be-determined constants. Similar to BFB 9/7 with Condition EP1, eight nonlinear equations are generated from (98) and (1). Again, with another application of the method of Lagrange multiplier, all 7 coefficients of  $F_4$  and  $G_3$  in (96)–(97) and 2 constants  $C_0$  and  $C_1$  in (98) are determined and listed in the follows

$$\begin{aligned}
a_1 &= .9593321752494364, & a_2 &= 12.2162082406675360, \\
a_3 &= -24.4791147610354754, & a_4 &= 22.6398493240698941, \\
b_1 &= 3.0406678247505636, & b_2 &= -5.1332187191964663, \\
b_3 &= 12.2581453031028809, & C_0 &= -68.0515225967840965, \\
C_1 &= -34.6903203318505382.
\end{aligned}$$

These coefficients, consequently, give rise to the BFB in Table 11.

Weights of the BFB 13/11 with Condition EP1 are calculated by using (35)–(40) and (41)–(46), and are tabulated in Table 12, and graphs of  $\phi_{13,11}^{EP1}$ ,  $\psi_{13,11}^{EP1}$ ,  $\tilde{\phi}_{13,11}^{EP1}$ , and  $\tilde{\psi}_{13,11}^{EP1}$  are plotted in Fig. 5.

### 5.6. BFB 13/11 with Condition EP2: $m = 2$ and $n = 4$ .

The biorthogonal refinable functions and wavelets are denoted by  $\phi_{13,11}^{EP2}$ ,  $\psi_{13,11}^{EP2}$ ,  $\tilde{\phi}_{13,11}^{EP2}$ , and  $\tilde{\psi}_{13,11}^{EP2}$ .

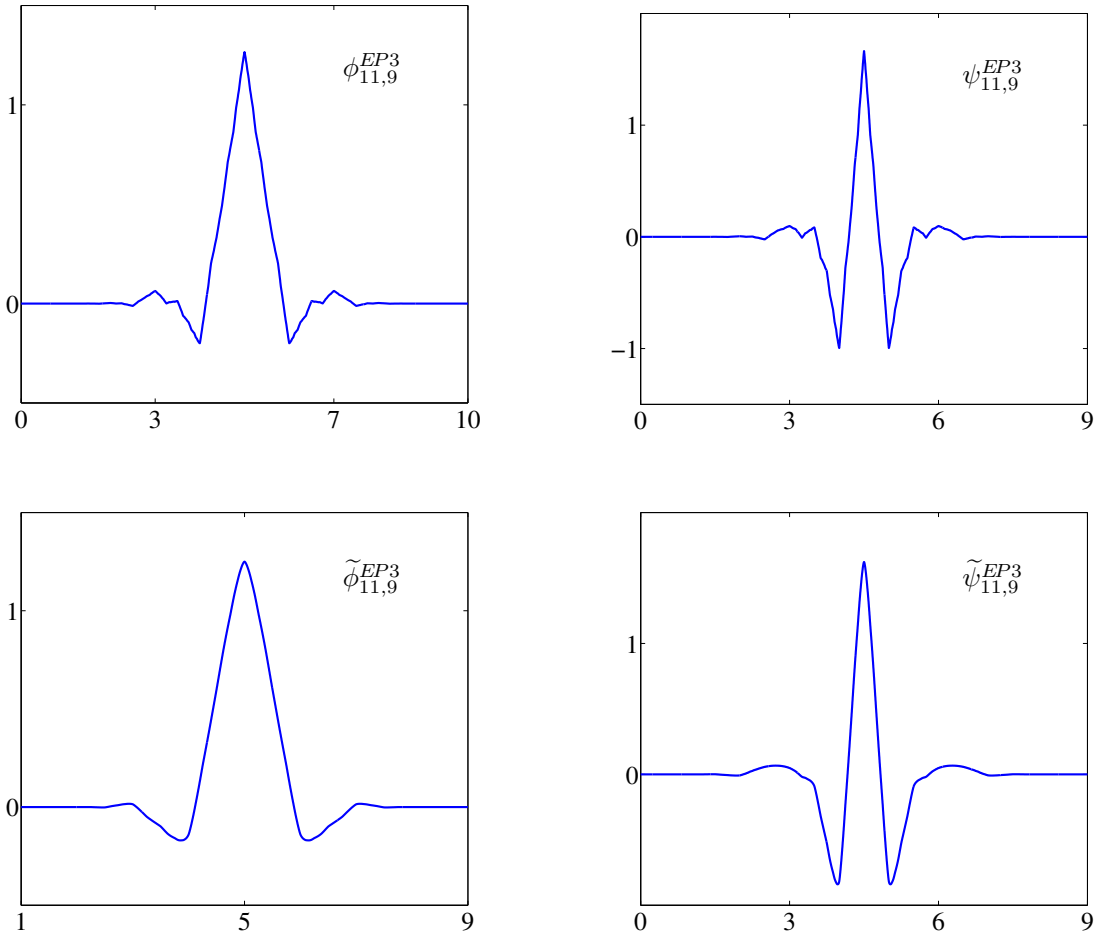


Figure 4. Plots of refinable functions and wavelets for BFB 11/9 with Condition EP3:  $\phi_{11,9}^{EP3}$ ,  $\psi_{11,9}^{EP3}$ ,  $\tilde{\phi}_{11,9}^{EP3}$ , and  $\tilde{\psi}_{11,9}^{EP3}$ .

Similar to BFB 13/11 with Condition EP1, write  $F_4$  and  $G_3$  as in (96)–(97). It then naturally follows from (98) and (1) that the coefficients of  $F_4$  and  $G_3$  in (96)–(97) are

$$\begin{aligned} a_1 &= .9606616521702165, & a_2 &= 12.3210523814804282, \\ a_3 &= -24.8502477444418170, & a_4 &= 23.0390962745854443; \\ b_1 &= 3.0393383478297835, & b_2 &= -5.2408281802108841, \\ b_3 &= 12.4370634141304899; & C_0 &= -69.2965856199102679, \\ C_1 &= -35.8173376714095869. \end{aligned}$$

The BFB 13/11 with Condition EP2 is now established, with all filters being listed in Table 13.

Weights of the BFB 13/11 with Condition EP2 are included in Table 14; and the graphs of  $\phi_{13,11}^{EP2}$ ,  $\psi_{13,11}^{EP2}$ ,  $\tilde{\phi}_{13,11}^{EP2}$ , and  $\tilde{\psi}_{13,11}^{EP2}$  are plotted in Fig. 6.

Table 11. BFB 13/11 with Condition EP1

$k$	$\mathbf{h}$	$\mathbf{g}$	$k$
0, 12	.0078167924717244	.0169293313839728	0, 10
1, 11	.0025401505134383	.0055013677237460	1, 9
2, 10	.0155045979503007	.0164019070423589	2, 8
3, 9	-.0288188979943560	-.0679969256352202	3, 7
4, 8	-.0863780693064859	-.3868846290196054	4, 6
5, 7	.3798321380741915	.8320978970094958	5
6	.8332201389554692		
$k$	$\tilde{\mathbf{h}}$	$\tilde{\mathbf{g}}$	$k$
1, 11	-.0169293313839728	.0078167924717244	-1, 11
2, 10	.0055013677237460	-.0025401505134383	0, 10
3, 9	-.0164019070423589	.0155045979503007	1, 9
4, 8	-.0679969256352202	.0288188979943560	2, 8
5, 7	.3868846290196054	-.0863780693064859	3, 7
6	.8320978970094958	-.3798321380741915	4, 6
		.8332201389554692	5

Table 12. Weights of BFB 13/11 with Condition EP1

Weights	$\mathbf{h}$	$\tilde{\mathbf{h}}$	Weights
$w_{0,0}$	1.0000000000000000	1.0021652860677171	$\tilde{w}_{0,0}$
$w_{0,1}$	1.0021652860677171	1.0000000000000000	$\tilde{w}_{0,1}$
$w_{1,0}$	.9691101165459206	1.0337693640811553	$\tilde{w}_{1,0}$
$w_{1,1}$	1.0333369523914061	.9729356908868231	$\tilde{w}_{1,1}$
$w_{2,0}$	.9480793557865392	1.0561556123339834	$\tilde{w}_{2,0}$
$w_{2,1}$	.9922475548642841	1.0135738984465527	$\tilde{w}_{2,1}$
$w_{3,0}$	.9407923016330405	1.0642030540923618	$\tilde{w}_{3,0}$
$w_{3,1}$	.9569019736628954	1.0498050885055738	$\tilde{w}_{3,1}$

### 5.7. BFB 15/13 with Condition EP2: $m = 3$ and $n = 4$ .

The biorthogonal refinable functions and wavelets are denoted by  $\phi_{15,13}^{EP2}$ ,  $\psi_{15,13}^{EP2}$ ,  $\tilde{\phi}_{15,13}^{EP2}$ , and  $\tilde{\psi}_{15,13}^{EP2}$ . With  $F_4$  and  $G_3$  in (96)–(97), and by using (58), the identity that  $F_4$  and  $G_3$  must satisfy

$$F_4(t)G_3(t) = 1 + 6t + 21t^2 + 56t^3 + 126t^4 + 252t^5 + C_0t^6(1 - 2t), \quad (99)$$

for some constant  $C_0$ . Again, by using (98) and (2), the 8 coefficients  $a_1, a_2, \dots, C_0$  in (96)–(97) and (99) are

$$\begin{aligned} a_1 &= 3.6479393214173282, & a_2 &= 9.1438541182872717, \\ a_3 &= -4.7482443902585054, & a_4 &= 7.6579720661169862; \\ b_1 &= 2.3520606785826718, & b_2 &= 3.2759712459514760, \\ b_3 &= 27.2908003439998804; & C_0 &= -104.4960933481634606, \end{aligned}$$

which gives rise to the BFB 15/13 with Condition EP2 in Table 15.

Weights of the BFB 15/13 with Condition EP2 are in Table 16. Graphs of  $\phi_{15,13}^{EP2}$ ,  $\psi_{15,13}^{EP2}$ ,  $\tilde{\phi}_{15,13}^{EP2}$ , and  $\tilde{\psi}_{15,13}^{EP2}$  are plotted in Fig. 7.

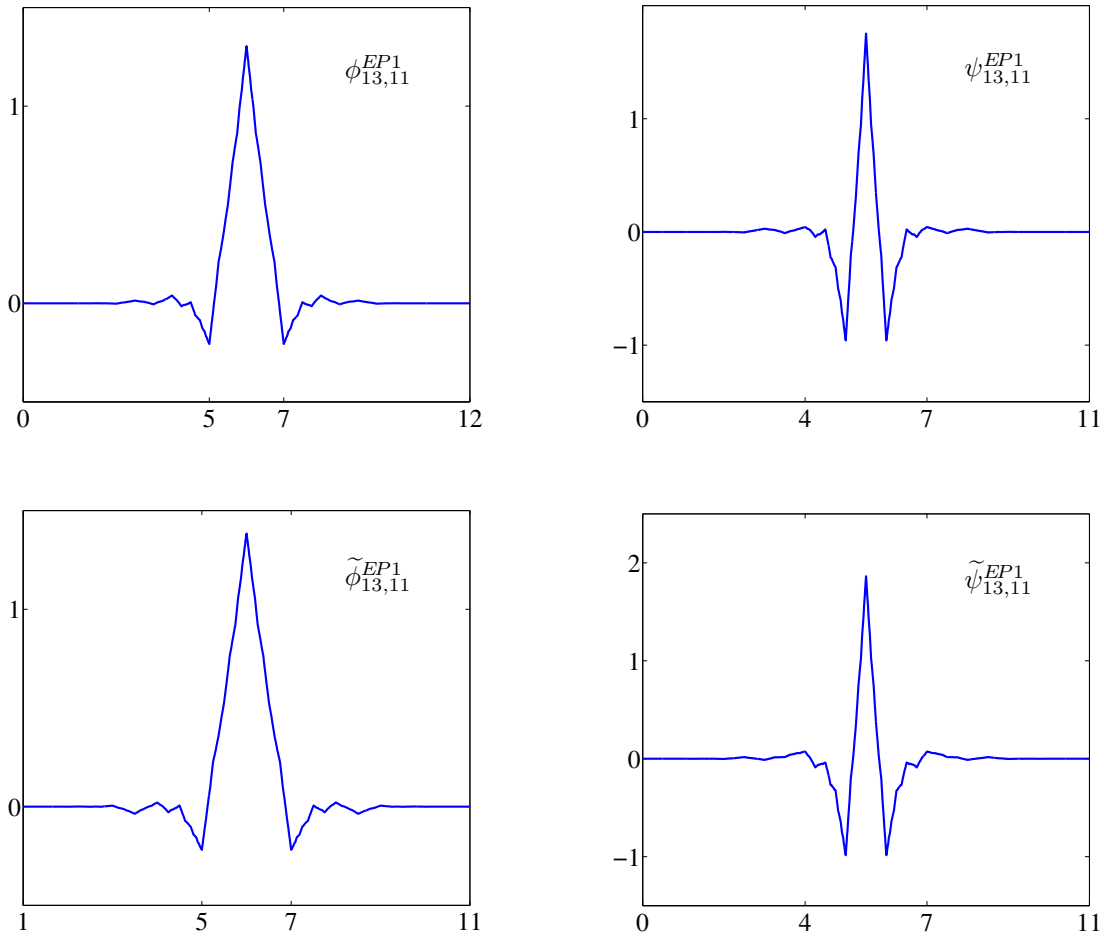


Figure 5. Plots of refinable functions and wavelets for BFB 13/11 with Condition EP1:  $\phi_{13,11}^{EP1}$ ,  $\psi_{13,11}^{EP1}$ ,  $\tilde{\phi}_{13,11}^{EP1}$ , and  $\tilde{\psi}_{13,11}^{EP1}$ .

### 5.8. BFB 15/13 with Condition EP3: $m = 3$ and $n = 4$ .

The biorthogonal refinable functions and wavelets are denoted by  $\phi_{15,13}^{EP3}$ ,  $\psi_{15,13}^{EP3}$ ,  $\tilde{\phi}_{15,13}^{EP3}$ , and  $\tilde{\psi}_{15,13}^{EP3}$ . The two polynomials  $F_4$  and  $G_3$ , again, can be expressed by (96)–(97), along with the identity (99) they must satisfy. With (99) and (3), we have all coefficients in (96)–(97) as

$$\begin{aligned} a_1 &= 2.2984779015187734, & a_2 &= 3.3402901113058788, \\ a_3 &= 25.1604546292217135, & a_4 &= 8.1821330613446772; \\ b_1 &= 3.7015220984812266, & b_2 &= 9.1518431433516251, \\ b_3 &= -2.5599215147185578; & C_0 &= 10.4728092300131280. \end{aligned}$$

Hence, this The new BFB 15/13 with Condition EP3 is listed in Table 17. Weights of the BFB 15/13 with Condition EP3 are posted in Table 18.

Graphs of their corresponding refinable functions and wavelets,  $\phi_{15,13}^{EP3}$ ,  $\psi_{15,13}^{EP3}$ ,  $\tilde{\phi}_{15,13}^{EP3}$ , and  $\tilde{\psi}_{15,13}^{EP3}$  are plotted in Fig. 8.

Table 13. BFB 13/11 with Condition EP2

$k$	$\mathbf{h}$	$\mathbf{g}$	$k$
0, 12	.0079546392618013	.0171764294495679	0, 10
1, 11	.0025013232150223	.0054010999517869	1, 9
2, 10	.0153343593296121	.0156312352785074	2, 8
3, 9	-.0287317936661742	-.0675370994132515	3, 7
4, 8	-.0869964910685564	-.3863610553213491	4, 6
5, 7	.3797838610444257	.8313787801094767	5
6	.8345217661408334		
$k$	$\tilde{\mathbf{h}}$	$\tilde{\mathbf{g}}$	$k$
1, 11	-.0171764294495679	.0079546392618013	-1, 11
2, 10	.0054010999517869	-.0025013232150223	0, 10
3, 9	-.0156312352785074	.0153343593296121	1, 9
4, 8	-.0675370994132515	.0287317936661742	2, 8
5, 7	.3863610553213491	-.0869964910685564	3, 7
6	.8313787801094767	-.3797838610444257	4, 6
		.8345217661408334	5

Table 14. Weights of BFB 13/11 with Condition EP2

Weights	$\mathbf{h}$	$\tilde{\mathbf{h}}$	Weights
$w_{0,0}$	1.0022953021927952	1.0000000000000000	$\tilde{w}_{0,0}$
$w_{0,1}$	1.0000000000000000	1.0022953021927952	$\tilde{w}_{0,1}$
$w_{1,0}$	.9722152774656418	1.0306138911543154	$\tilde{w}_{1,0}$
$w_{1,1}$	1.0348547593000506	.9717849441532523	$\tilde{w}_{1,1}$
$w_{2,0}$	.9512382279231992	1.0527195851470402	$\tilde{w}_{2,0}$
$w_{2,1}$	.9953879658869954	1.0107808048799724	$\tilde{w}_{2,1}$
$w_{3,0}$	.9439283959214199	1.0606965102716203	$\tilde{w}_{3,0}$
$w_{3,1}$	.9602096683055518	1.0465689771764431	$\tilde{w}_{3,1}$

### 5.9. BFB 17/15 with Condition EP2: $m = 3$ and $n = 5$ .

Denote by  $\phi_{17,15}^{EP2}$ ,  $\psi_{17,15}^{EP2}$ ,  $\tilde{\phi}_{17,15}^{EP2}$ , and  $\tilde{\psi}_{17,15}^{EP2}$ , the refinable functions and wavelets. With

$$F_5(t) = 1 + a_1t + a_2t^2 + a_3t^3 + a_4t^4 + a_5t^5, \quad (100)$$

$$G_4(t) = 1 + b_1t + b_2t^2 + b_3t^3 + b_4t^4, \quad (101)$$

the identity that  $F_5$  and  $G_4$  must satisfy is

$$F_5(t)G_4(t) = 1 + 6t + 21t^2 + 56t^3 + 126t^4 + 252t^5 + t^6(1 - 2t)(C_0 + C_1(1 - 2t)^2), \quad (102)$$

for some constants  $C_0$  and  $C_1$ . Again, the requirements (102) and (2), plus another application of the method of Lagrange multiplier, lead to the coefficients in (100)–(101) as

$$\begin{aligned} a_1 &= 3.6850326693942465, & a_2 &= 8.8887467265749782, \\ a_3 &= -11.9308411108643810, & a_4 &= 12.6664830888352934, \\ a_5 &= 23.4927022045793695; \end{aligned}$$



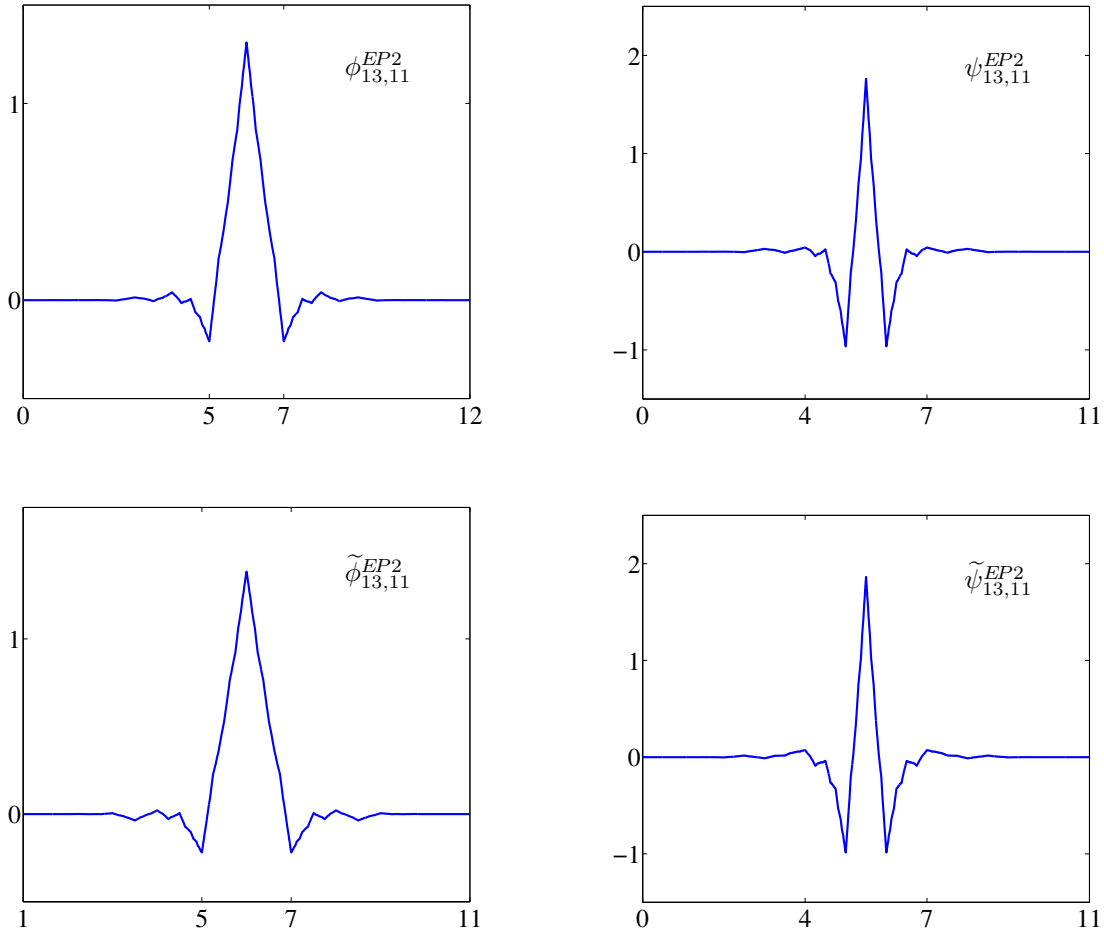


Figure 6. Plots of refinable functions and wavelets for BFB 13/11 with Condition EP2:  $\phi_{13,11}^{EP2}$ ,  $\psi_{13,11}^{EP2}$ ,  $\tilde{\phi}_{13,11}^{EP2}$ , and  $\tilde{\psi}_{13,11}^{EP2}$ .

and

$$\begin{aligned} b_1 &= 2.3149673306057535, & b_2 &= 3.5805230315624288, \\ b_3 &= 34.1593384839883973, & b_4 &= -16.7516163451564283; \\ C_0 &= -505.9056340980933762, & C_1 &= 49.1925917802655278. \end{aligned}$$

All these coefficients consequently yield the BFB 17/15 with Condition EP2, being listed in Table 19.

Weights of the BFB 17/15 with Condition EP2 are in Table 20; and graphs of  $\phi_{17,15}^{EP2}$ ,  $\psi_{17,15}^{EP2}$ ,  $\tilde{\phi}_{17,15}^{EP2}$ , and  $\tilde{\psi}_{17,15}^{EP2}$  are plotted in Fig. 9.

All Riesz bounds of these new BFBs with certain EP conditions are calculated and listed in Table 21, by using Proposition 1 in Appendix I, where the lower Riesz bounds (LRB) and upper Riesz bounds (URB) for both LeGall 5/3 and CDF 9/7 are also included for reference.

Table 15. BFB 15/13 with Condition EP2

$k$	$\mathbf{h}$	$\mathbf{g}$	$k$
0, 14	.0006610112277940	-.0094226122984621	0, 12
1, 13	.0003173895595891	-.0045243388339540	1, 11
2, 12	.0093232275587282	.0525909291493993	2, 10
3, 11	.0032000219790237	.0434496188269085	3, 9
4, 10	-.0904474953662203	-.0969250629132126	4, 8
5, 9	-.0442917369506223	-.3924786705862283	5, 7
6, 8	.4340166471729719	.8146202733110984	6
7	.7886554320105664		
$k$	$\tilde{\mathbf{h}}$	$\tilde{\mathbf{g}}$	$k$
1, 13	-.0094226122984621	-.0006610112277940	-1, 13
2, 12	.0045243388339540	.0003173895595891	0, 12
3, 11	.0525909291493993	-.0093232275587282	1, 11
4, 10	-.0434496188269085	.0032000219790237	2, 10
5, 9	-.0969250629132126	.0904474953662203	3, 9
6, 8	.3924786705862283	-.0442917369506223	4, 8
7	.8146202733110984	-.4340166471729719	5, 7
		.7886554320105664	6

Table 16. Weights of BFB 15/13 with Condition EP2

Weights	$\mathbf{h}$	$\tilde{\mathbf{h}}$	Weights
$w_{0,0}$	1.0191987060160679	1.0000000000000000	$\tilde{w}_{0,0}$
$w_{0,1}$	1.0000000000000000	1.0191987060160679	$\tilde{w}_{0,1}$
$w_{1,0}$	1.0776869258063536	.9418685936641299	$\tilde{w}_{1,0}$
$w_{1,1}$	.9857716654214979	1.0813468364854223	$\tilde{w}_{1,1}$
$w_{2,0}$	1.0967326329441575	.9236485338394675	$\tilde{w}_{2,0}$
$w_{2,1}$	1.0792592488226427	.9769729448918817	$\tilde{w}_{2,1}$
$w_{3,0}$	1.1016426945108856	.9189712518338777	$\tilde{w}_{3,0}$
$w_{3,1}$	1.1108518864873426	.9431374022762024	$\tilde{w}_{3,1}$

## 6. Smoothness of Refinable Functions and Wavelets

The smoothness of all 9 new pairs of biorthogonal refinable functions and wavelets  $(\phi, \psi)$  and  $(\tilde{\phi}, \tilde{\psi})$  constructed in Section V can be described and determined by the *Hölder exponents* of the refinable function. A function  $f$  is said to have *Hölder exponent*  $\nu = n + \alpha$ , with  $n$  being a nonnegative integer and  $0 \leq \alpha < 1$ , and can be denoted by  $f \in \mathbb{C}^\nu(\mathbb{R})$ , if  $f \in \mathbb{C}^n(\mathbb{R})$ , i.e.,  $f$  is  $n$ -th order differentiable, and

$$|f^{(n)}(u) - f^{(n)}(v)| \leq C |u - v|^\alpha, \quad u, v \in \mathbb{R},$$

where  $C$  is a positive constant.

All the Hölder exponents of the nine biorthogonal pairs of refinable functions we have established are listed in Table 22, where, for additional information, the numbers of VM for all nine biorthogonal wavelets are also included in the fourth column of the table.

The Hölder exponents for LeGall 5/3  $(\phi^{53}, \psi^{53})$  and  $(\tilde{\phi}^{53}, \tilde{\psi}^{53})$  and CDF 9/7  $(\phi^{97}, \psi^{97})$  and

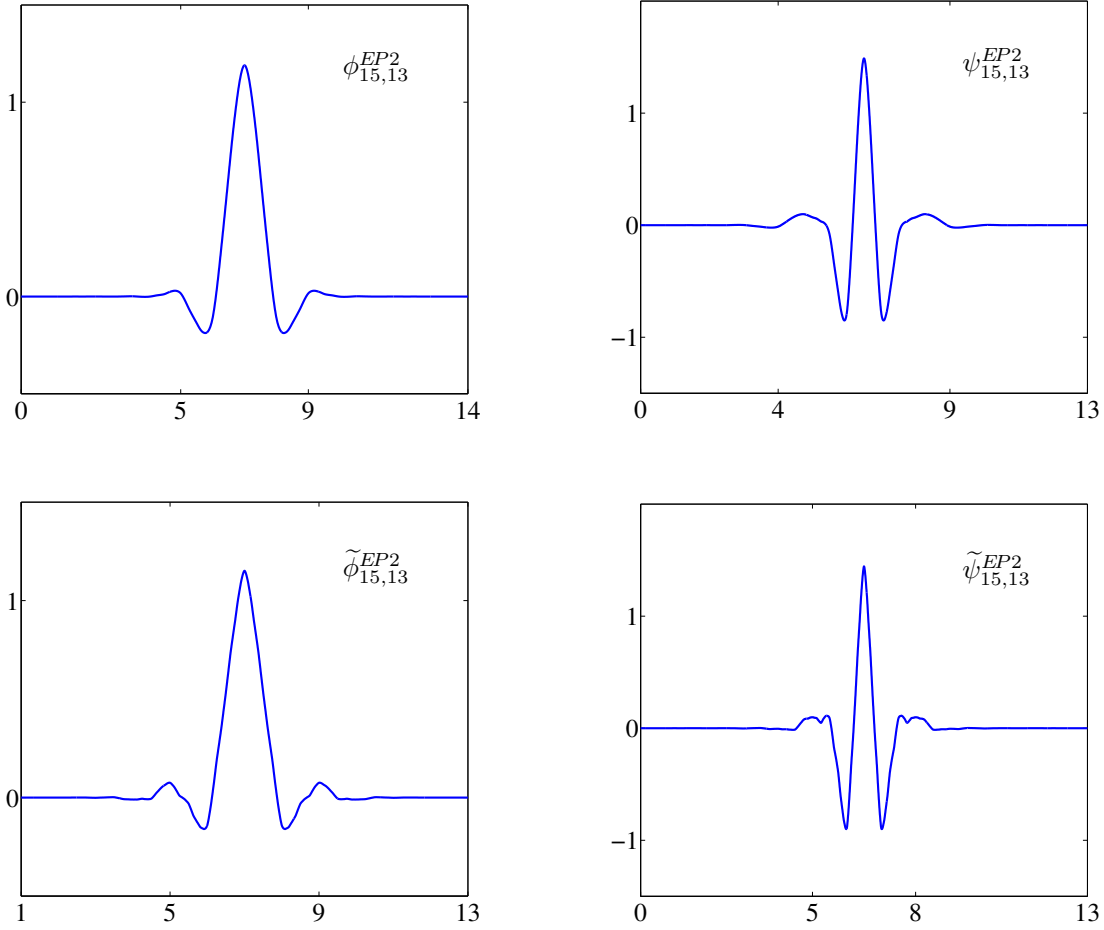


Figure 7. Plots of refinable functions and wavelets for BFB 15/13 with Condition EP2:  $\phi_{15,13}^{EP2}$ ,  $\psi_{15,13}^{EP2}$ ,  $\tilde{\phi}_{15,13}^{EP2}$ , and  $\tilde{\psi}_{15,13}^{EP2}$ .

$(\tilde{\phi}^{97}, \tilde{\psi}^{97})$  were also included in Table 22 for comparison purposes. The negative value of the Hölder exponent for  $\phi^{53}$  indicates that the corresponding refinable function  $\phi^{53}$  was discontinuous.

## 7. Image Coding Performance Analysis

Energy compaction, as an important property, can be used to assess the coding efficiency of a transform. A transform with strong energy compaction property is desired for data compression applications. Here, to evaluate coding performance of wavelet transform with a specific set of filterbanks, we calculate the transform's *potential energy compaction* (PEC) (Hamou and El-Sakka, 2003)

$$\text{Potential Energy Compaction (PEC)} = \frac{1}{M} \sum_{n=0}^M x_n^2, \quad (103)$$

where  $x$  represents the coefficients in all of the high frequency subbands and  $M$  is the total number of such coefficients. PEC is a direct indicator of energy compaction property for a

Table 17. BFB 15/13 with Condition EP3

$k$	$\mathbf{h}$	$\mathbf{g}$	$k$
0, 14	.0007062550991513	.0008838563781069	0, 12
1, 13	-.0100995844590737	-.0126393170840225	1, 11
2, 12	.0010818920605614	-.0004727179798768	2, 10
3, 11	.0571264253782391	.0976137198571110	3, 9
4, 10	-.0361757858198670	-.0370670250452229	4, 8
5, 9	-.1066062518195251	-.4385277933663622	5, 7
6, 8	.3879410292534281	.7804185544805331	6
7	.8262656029872668		
$k$	$\tilde{\mathbf{h}}$	$\tilde{\mathbf{g}}$	$k$
1, 13	.0008838563781069	-.0007062550991513	-1, 13
2, 12	.0126393170840225	-.0100995844590737	0, 12
3, 11	-.0004727179798768	-.0010818920605614	1, 11
4, 10	-.0976137198571110	.0571264253782391	2, 10
5, 9	-.0370670250452229	.0361757858198670	3, 9
6, 8	.4385277933663622	-.1066062518195251	4, 8
7	.7804185544805331	-.3879410292534281	5, 7
		.8262656029872668	6

Table 18. Weights of BFB 15/13 with Condition EP3

Weights	$\mathbf{h}$	$\tilde{\mathbf{h}}$	Weights
$w_{0,0}$	1.0157926905885902	1.0157926905885902	$\tilde{w}_{0,0}$
$w_{0,1}$	1.0157926905885902	1.0157926905885902	$\tilde{w}_{0,1}$
$w_{1,0}$	.9514641687951524	1.0783320075958603	$\tilde{w}_{1,0}$
$w_{1,1}$	1.1173065448109509	.9934809219211633	$\tilde{w}_{1,1}$
$w_{2,0}$	.9310991607803551	1.0984191634975949	$\tilde{w}_{2,0}$
$w_{2,1}$	1.0007436172766918	1.0937005405721780	$\tilde{w}_{2,1}$
$w_{3,0}$	.9257638157233974	1.1036000188435020	$\tilde{w}_{3,0}$
$w_{3,1}$	.9626051964723454	1.1269848896338305	$\tilde{w}_{3,1}$

wavelet transform. The compression efficiency will be inversely proportional to the PEC rating. We compared the PEC values of our newly constructed BFBs to those of CDF 5/3 and CDF 9/7 on four different images (as shown in Fig. 10), and the results are tabulated in Table 23. From the results, we can see that BFB 15/13 with EP3 gives the smallest PEC values for all of the six images. In fact, BFB 11/9 with EP3 and CDF 9/7 produce similar PEC values as BFB 15/13 with EP3 does, which indicates that all of the three filterbanks shall demonstrate comparable compression performance, with BFB 15/13 with EP3 performs little better than the other two. This can be proven with real image compression results, which is tabulated in Table 24. Some image examples are shown in Fig. 10.

## 8. Conclusion

Weights within the energy of lowpass and highpass filters derived from a pair of compactly supported biorthogonal refinable functions and wavelets are re-defined and re-formulated. The recently newly introduced notion energy preservation (EP) is further investigated in detail. Exten-

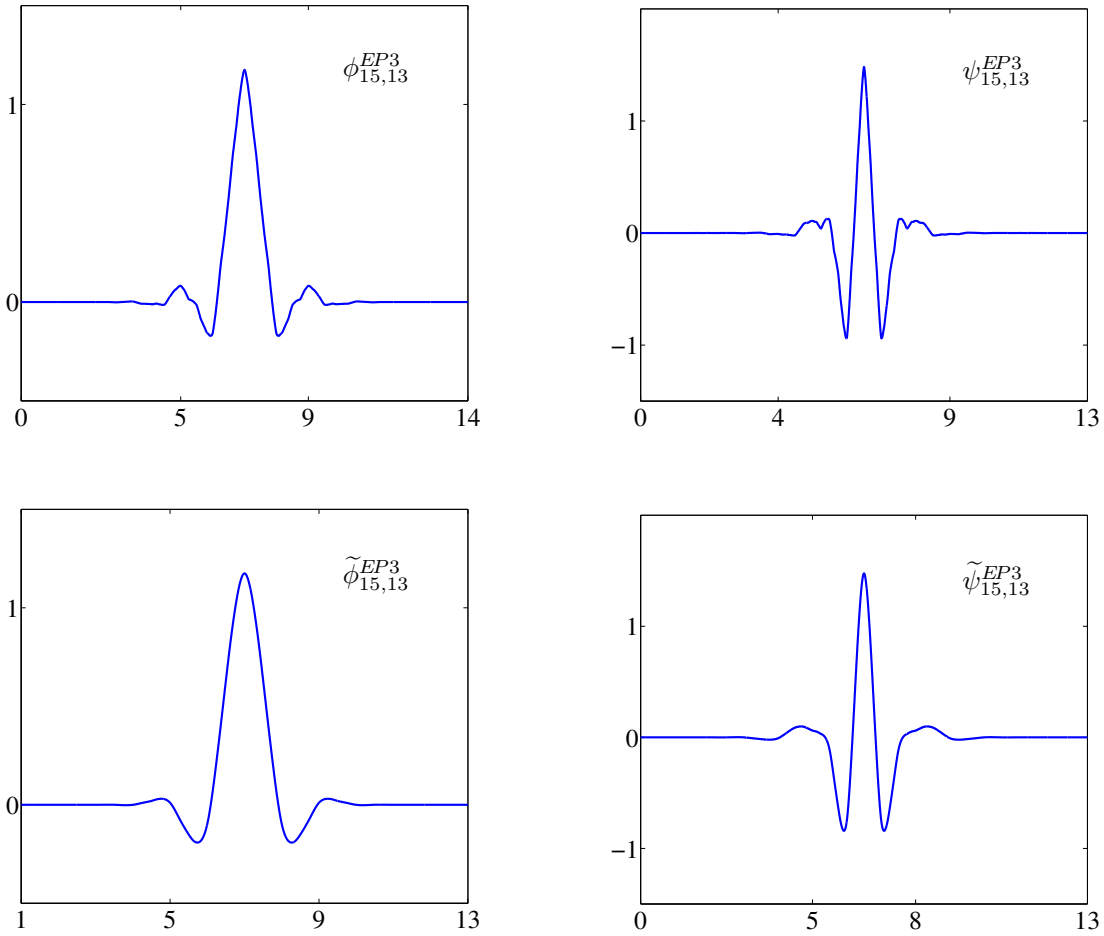


Figure 8. Plots of refinable functions and wavelets for BFB 15/13 with Condition EP3:  $\phi_{15,13}^{EP3}$ ,  $\psi_{15,13}^{EP3}$ ,  $\tilde{\phi}_{15,13}^{EP3}$ , and  $\tilde{\psi}_{15,13}^{EP3}$ .

sive examples of biorthogonal filterbanks (BFB) with PR FIR QMF were established, by using the efficient construction algorithm. It is worth mentioning that there is no other choice to improve the performance of a PR FIR QMF system but make the length of each filter *longer* in order to have all desirable features when applied to image processing. These features include, but may not be limited to, the high number of vanishing moments (VM), the symmetry or linear-phase, FIR, and, very substantially, the Condition EP proposed in this paper. Meanwhile, it is still immature with regard to how to choose one of the four EP conditions over the others. For a fixed VM of  $2m$ , one or two of the EP conditions may not yield any solution. To demonstrate the performance of these new BFB  $m/n$ 's with Condition EPs, their potential energy compaction (PEC) values are evaluated and compared to those of CDF 5/3 and CDF 9/7, and, also for comparison purposes, they are applied to four typical images for demonstrating their image coding performance.

Table 19. BFB 17/15 with Condition EP2

$k$	$\mathbf{h}$	$\mathbf{g}$	$k$
0, 16	-.0005069534007951	.0014459450089716	0, 14
1, 15	.0031211432035101	-.0089022017217417	1, 13
2, 14	.0019326663143561	-.0121746705835542	2, 12
3, 13	-.0033297529577634	.0505145928320875	3, 11
4, 12	.0027378744569749	.0569052890877736	4, 10
5, 11	-.0680690006051480	-.0916641029662372	5, 9
6, 10	-.0505086931108201	-.3997299541064647	6, 8
7, 9	.4218310009526751	.8072102048983305	7
8	.7997969926671159		
$k$	$\tilde{\mathbf{h}}$	$\tilde{\mathbf{g}}$	$k$
1, 15	-.0014459450089716	-.0005069534007951	-1, 15
2, 14	-.0089022017217417	-.0031211432035101	0, 14
3, 13	.0121746705835542	.0019326663143561	1, 13
4, 12	.0505145928320875	.0033297529577634	2, 12
5, 11	-.0569052890877736	.0027378744569749	3, 11
6, 10	-.0916641029662372	.0680690006051480	4, 10
7, 9	.3997299541064647	-.0505086931108201	5, 9
8	.8072102048983305	-.4218310009526751	6, 8
		.7997969926671159	7

Table 20. Weights of BFB 17/15 with Condition EP2

Weights	$\mathbf{h}$	$\tilde{\mathbf{h}}$	Weights
$w_{0,0}$	1.0099916839491913	1.0000000000000000	$\tilde{w}_{0,0}$
$w_{0,1}$	1.0000000000000000	1.0099916839491913	$\tilde{w}_{0,1}$
$w_{1,0}$	1.0643121756317232	.9457021959789806	$\tilde{w}_{1,0}$
$w_{1,1}$	.9709123773677931	1.0685914739068977	$\tilde{w}_{1,1}$
$w_{2,0}$	1.0842075968188536	.9272365112295471	$\tilde{w}_{2,0}$
$w_{2,1}$	1.0568817300321149	.9743135751774849	$\tilde{w}_{2,1}$
$w_{3,0}$	1.0895329160787905	.9224913670893828	$\tilde{w}_{3,0}$
$w_{3,1}$	1.0901047307450765	.9406097856641525	$\tilde{w}_{3,1}$

## APPENDIX I

## Evaluation of Euler-Frobenius Polynomials

For a refinable function  $\phi$ , its integer-translates  $\{\phi(\cdot - k) : k \in \mathbb{Z}\}$  constitutes a Riesz basis. Its *autocorrelation symbol* or *Euler-Frobenius polynomial* is

$$\Phi(z) = \sum_{k \in \mathbb{Z}} \langle \phi(\cdot), \phi(\cdot - k) \rangle z^k. \quad (104)$$

It is also known that, in terms of Fourier transforms,

$$\Phi(e^{-j\omega}) = \sum_{k \in \mathbb{Z}} \left| \hat{\phi}(\omega + 2\pi k) \right|^2, \quad \omega \in \mathbb{R}. \quad (105)$$

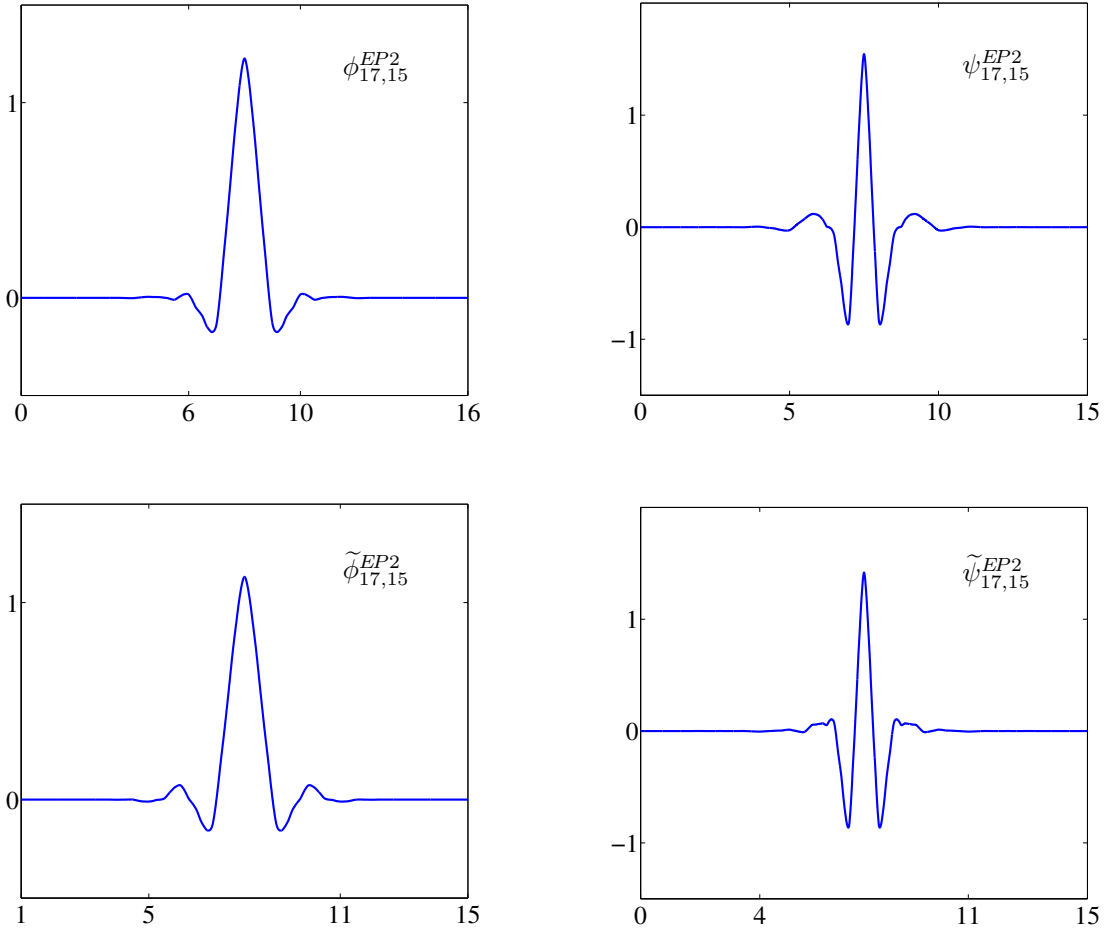


Figure 9. Plots of refinable functions and wavelets for BFB 17/15 with Condition EP2:  $\phi_{17,15}^{EP2}$ ,  $\psi_{17,15}^{EP2}$ ,  $\tilde{\phi}_{17,15}^{EP2}$ , and  $\tilde{\psi}_{17,15}^{EP2}$ .

Similarly, let  $\tilde{\Phi}$ ,  $\tilde{\Psi}$ , and  $\tilde{\Psi}$  be the Euler-Frobenius polynomials for  $\tilde{\phi}$ ,  $\tilde{\psi}$ , and  $\tilde{\phi}$ ; and introduce

$$\Theta(z) = \sum_{k \in \mathbb{Z}} \langle \phi(\cdot), \psi(\cdot - k) \rangle z^k, \quad (106)$$

$$\tilde{\Theta}(z) = \sum_{k \in \mathbb{Z}} \langle \tilde{\phi}(\cdot), \tilde{\psi}(\cdot - k) \rangle z^k. \quad (107)$$

Then, with the notation in (11), all two-scale relations and Fourier transforms lead us to the following matrix identity

$$M_{H,G}(z) \begin{bmatrix} \Phi(z) & 0 \\ 0 & \Phi(-z) \end{bmatrix} M_{H,G}(z)^* = \begin{bmatrix} \Phi(z^2) & \Theta(z^2) \\ \overline{\Theta(z^2)} & \Psi(z^2) \end{bmatrix}, \quad |z| = 1, \quad (108)$$

which is equivalent to

$$|H(z)|^2 \Phi(z) + |H(-z)|^2 \Phi(-z) = \Phi(z^2), \quad (109)$$

$$|G(z)|^2 \Phi(z) + |G(-z)|^2 \Phi(-z) = \Psi(z^2), \quad (110)$$

$$H(z) \overline{G(z)} \Phi(z) + H(-z) \overline{G(-z)} \Phi(-z) = \Theta(z^2). \quad (111)$$

Table 21. Lower Riesz Bounds (LRB) and Upper Riesz Bounds (URB) of all New Biorthogonal Refinable Functions and Wavelets in Section 5 & with LRBs and URBs for LeGall 5/3 and CDF 9/7

	LRB	URB	LRB	URB	
$\Phi_{7,5}^{EP4}$	.9875	1.0123	.9884	1.0125	$\tilde{\Phi}_{7,5}^{EP4}$
$\Psi_{7,5}^{EP4}$	.9833	1.0369	.9648	1.0187	$\tilde{\Psi}_{7,5}^{EP4}$
$\Phi_{9,7}^{EP1}$	.9983	1.0018	.9982	1.0017	$\tilde{\Phi}_{9,7}^{EP1}$
$\Psi_{9,7}^{EP1}$	.9948	1.0024	.9976	1.0052	$\tilde{\Psi}_{9,7}^{EP1}$
$\Phi_{9,7}^{EP2}$	.9983	1.0019	.9982	1.0017	$\tilde{\Phi}_{9,7}^{EP2}$
$\Psi_{9,7}^{EP2}$	.9948	1.0024	.9976	1.0052	$\tilde{\Psi}_{9,7}^{EP2}$
$\Phi_{11,9}^{EP3}$	.9031	1.1135	.8917	1.1011	$\tilde{\Phi}_{11,9}^{EP3}$
$\Psi_{11,9}^{EP3}$	.7329	1.1531	.8713	1.3549	$\tilde{\Psi}_{11,9}^{EP3}$
$\Phi_{13,11}^{EP1}$	.9525	1.0663	.9368	1.0488	$\tilde{\Phi}_{13,11}^{EP1}$
$\Psi_{13,11}^{EP1}$	.9221	1.0801	.9255	1.0837	$\tilde{\Psi}_{13,11}^{EP1}$
$\Phi_{13,11}^{EP2}$	.9511	1.0627	.9399	1.0504	$\tilde{\Phi}_{13,11}^{EP2}$
$\Psi_{13,11}^{EP2}$	.9185	1.0827	.9233	1.0879	$\tilde{\Psi}_{13,11}^{EP2}$
$\Phi_{15,13}^{EP2}$	.8643	1.1234	.8834	1.1447	$\tilde{\Phi}_{15,13}^{EP2}$
$\Psi_{15,13}^{EP2}$	.8643	1.4217	.6959	1.1447	$\tilde{\Psi}_{15,13}^{EP2}$
$\Phi_{15,13}^{EP3}$	.8638	1.2021	.8173	1.1442	$\tilde{\Phi}_{15,13}^{EP3}$
$\Psi_{15,13}^{EP3}$	.6329	1.2021	.8173	1.5521	$\tilde{\Psi}_{15,13}^{EP3}$
$\Phi_{17,15}^{EP2}$	.8949	1.1052	.9003	1.1119	$\tilde{\Phi}_{17,15}^{EP2}$
$\Psi_{17,15}^{EP2}$	.8768	1.3555	.7341	1.1352	$\tilde{\Psi}_{17,15}^{EP2}$
$\Phi^{53}$	.4675	1.7662	.5000	1.5000	$\tilde{\Phi}^{53}$
$\Psi^{53}$	.4416	1.7662	.5000	2.0000	$\tilde{\Psi}^{53}$
$\Phi^{97}$	.8920	1.1802	.8388	1.1085	$\tilde{\Phi}^{97}$
$\Psi^{97}$	.6757	1.2016	.8336	1.4650	$\tilde{\Psi}^{97}$

Evidently  $\Phi(z) = \Psi(z) = 1$  and  $\Theta(z) = 0$  when  $\phi$  is orthonormal. Certainly, with  $H$ ,  $G$ ,  $\Phi$ , and  $\Psi$  replaced by  $\tilde{H}$ ,  $\tilde{G}$ ,  $\tilde{\Phi}$ , and  $\tilde{\Psi}$ , (109)–(111) becomes

$$|\tilde{H}(z)|^2 \tilde{\Phi}(z) + |\tilde{H}(-z)|^2 \tilde{\Phi}(-z) = \tilde{\Phi}(z^2), \quad (112)$$

$$|\tilde{G}(z)|^2 \tilde{\Phi}(z) + |\tilde{G}(-z)|^2 \tilde{\Phi}(-z) = \tilde{\Psi}(z^2), \quad (113)$$

$$\tilde{H}(z) \overline{\tilde{G}(z)} \tilde{\Phi}(z) + \tilde{H}(-z) \overline{\tilde{G}(-z)} \tilde{\Phi}(-z) = \tilde{\Theta}(z^2). \quad (114)$$

The identities (109)–(111) and (112)–(114) are both convenient and ultrapractical for the evaluation of all Euler-Frobenius polynomials. For instance, for LeGall 5/3, a brusque calculation yields the following explicit expressions

$$\Phi^{53}(e^{-j\omega}) = 1 - \frac{201}{308} \cos \omega + \frac{9}{77} \cos 2\omega + \frac{1}{308} \cos 3\omega, \quad (115)$$

$$\tilde{\Phi}^{53}(e^{-j\omega}) = 1 + \frac{1}{2} \cos \omega, \quad (116)$$

$$\Psi^{53}(e^{-j\omega}) = \frac{12}{11} + \frac{51}{77} \cos \omega + \frac{1}{77} \cos 2\omega, \quad (117)$$

$$\tilde{\Psi}^{53}(e^{-j\omega}) = \frac{9}{8} - \frac{3}{4} \cos \omega + \frac{1}{8} \cos 2\omega, \quad (118)$$



Table 22. Hölder exponents of the nine BFBs

	$\phi$	$\tilde{\phi}$	VM of $\psi$ and $\tilde{\psi}$
BFB 7/5 EP4	.4814	.4117	2
BFB 9/7 EP1	.4149	.4476	2
BFB 9/7 EP2	.4179	.4189	2
BFB 11/9 EP3	.9722	1.4355	4
BFB 13/11 EP1	.8749	.8958	4
BFB 13/11 EP2	.8684	.8941	4
BFB 15/13 EP2	2.0958	1.5348	6
BFB 15/13 EP3	1.4099	2.3061	6
BFB 17/15 EP2	1.6633	1.6825	6
LeGall 5/3	-.0606	1.0000	2
CDF 9/7	.9496	1.5467	4

Table 23. Comparison of PEC in (103), with transform level being 5

image	Potential Energy Compaction (PEC)										
	LeGall 5/3	CDF 9/7	BFB 7/5 EP4	BFB 9/7 EP1	BFB 9/7 EP2	BFB 11/9 EP3	BFB 13/11 EP1	BFB 13/11 EP2	BFB 15/13 EP2	<b>BFB 15/13 EP3</b>	BFB 17/15 EP2
barbara	1743	924	1233	1153	1153	897	1023	1025	1449	<b>881</b>	1359
house	3573	2015	2434	2314	2314	1954	2128	2133	2855	<b>1952</b>	2715
lenna	1277	591	860	792	792	570	679	682	995	<b>552</b>	923
sandiego	2141	1074	1293	1225	1225	1033	1137	1141	1536	<b>1028</b>	1447

and

$$\Theta^{53}(e^{-j\omega}) = e^{-j\omega/2} \left( -\frac{89}{308} \cos \frac{\omega}{2} + \frac{87}{308} \cos \frac{3\omega}{2} + \frac{1}{154} \cos \frac{5\omega}{2} \right), \quad (119)$$

$$\tilde{\Theta}^{53}(e^{-j\omega}) = e^{-j\omega/2} \left( \frac{1}{4} \cos \frac{\omega}{2} - \frac{1}{4} \cos \frac{3\omega}{2} \right). \quad (120)$$

For comparison purposes, we plot all Euler-Frobenius polynomials for LeGall 5/3 and CDF 9/7 in Fig. 11:  $\Phi^{53}$  and  $\tilde{\Phi}^{53}$ ,  $\Phi^{97}$  and  $\tilde{\Phi}^{97}$ ,  $\Psi^{53}$  and  $\tilde{\Psi}^{53}$ ,  $\Psi^{97}$  and  $\tilde{\Psi}^{97}$ ,  $e^{j\omega/2}\Theta^{53}(e^{j\omega})$  and  $e^{j\omega/2}\tilde{\Theta}^{53}(e^{-j\omega})$ , and  $e^{j\omega/2}\Theta^{97}(e^{j\omega})$  and  $e^{j\omega/2}\tilde{\Theta}^{97}(e^{-j\omega})$ . The closer the  $|\Phi|$  and  $|\tilde{\Phi}|$  to one,  $|\Psi|$  and  $|\tilde{\Psi}|$  to one, and  $|\Theta|$  and  $|\tilde{\Theta}|$  to zero, the more near-orthogonal the  $\phi$  and  $\tilde{\phi}$  are.

In general, we establish an efficient procedure for finding all Euler-Frobenius polynomials of any BFB. First,  $\Phi$ ,  $\Psi$ , and  $\Theta$  are clearly reciprocal polynomials satisfying

$$\overline{\Phi(z)} = \Phi(z), \quad (121)$$

$$\overline{\Psi(z)} = \Psi(z), \quad (122)$$

$$\overline{\Theta(z)} = z^{-1}\Theta(z). \quad (123)$$

With  $t$  in (53),  $\Phi(z)$  is a polynomial of exact degree  $2m + 2n - 1$ , denoted by

$$U_{2m+2n-1}(t) = \Phi(z). \quad (124)$$



Figure 10. Test images and compression results. Top to bottom: barbara, house, lenna, and sandiego. Left to right: original, CDF 9/7 with SPIHT (Said and Pearlman, 1996) at 0.5 bpp, BFB 11/9 EP3 with SPIHT at 0.5 bpp, and BFB 15/13 EP3 with SPIHT at 0.5 bpp

Hence,

$$\Phi(-z) = U_{2m+2n-1}(1-t), \quad (125)$$

$$\Phi(z^2) = U_{2m+2n-1}(4t(1-t)). \quad (126)$$

Second, with  $H$  and  $\tilde{H}$  in (54)–(55), together with  $F$  and  $G$  satisfying (56), the identity (109) becomes

$$\begin{aligned} (1-t)^{2m} [F_n(t)]^2 U_{2m+2n-1}(t) + t^{2m} [F_n(1-t)]^2 U_{2m+2n-1}(1-t) \\ = U_{2m+2n-1}(4t(1-t)). \end{aligned} \quad (127)$$

Table 24. Comparison of rate-distortion performance with SPIHT (Said and Pearlman, 1996) algorithm, with bit rate being 0.5 bpp

Image	PSNR (dB)										
	LeGall 5/3	CDF 9/7	BFB 7/5 EP4	BFB 9/7 EP1	BFB 9/7 EP2	BFB 11/9 EP3	BFB 13/11 EP1	BFB 13/11 EP2	BFB 15/13 EP2	BFB 15/13 EP3	BFB 17/15 EP2
barbara	29.9	31.3	29.7	29.9	29.9	31.3	30.5	30.5	30.8	<b>31.8</b>	31
house	25.5	<b>25.9</b>	25.3	25.5	25.5	<b>25.9</b>	25.7	25.7	25.4	25.8	25.6
lenna	36.4	37.1	35.7	36	36	37.1	36.5	36.5	36.4	<b>37.2</b>	36.6
sandiego	23.4	23.9	23.3	23.4	23.4	23.9	23.6	23.6	23.5	<b>24</b>	23.7

*Theorem 1:* The polynomial  $U_{2m+2n-1}$  in (127) is unique with  $U_{2m+2n-1}(0) = 1$ , and determined by the Maclaurin polynomial of degree  $2m + 2n - 1$  of the following function

$$-t^{2m} \frac{[F_n(1-t)]^2}{(1-t)^{2m} [F_n(t)]^2} U_{2m+2n-1}(1-t) + \frac{1}{(1-t)^{2m} [F_n(t)]^2} U_{2m+2n-1}(4t(1-t)). \quad (128)$$

Similarly, the unique polynomial  $V_{2m+2n-3}(t) = \tilde{\Phi}(z)$  of degree  $2m + 2n - 3$  and satisfying  $V_{2m+2n-3}(0) = 1$  and

$$\begin{aligned} (1-t)^{2m} [G_{n-1}(t)]^2 V_{2m+2n-3}(t) + t^{2m} [G_{n-1}(1-t)]^2 V_{2m+2n-3}(1-t) \\ = V_{2m+2n-3}(4t(1-t)), \end{aligned} \quad (129)$$

can also be evaluated by Proposition 1. After both  $\Phi$  and  $\tilde{\Phi}$  are obtained,  $\Psi$ ,  $\tilde{\Psi}$ ,  $\Theta$  and  $\tilde{\Theta}$  can all be obtained by (110), (113), (111), and (114), respectively.

## APPENDIX II

### Additional BFBs

Table 25. BFB 7/5 with Condition EP1

$k$	$\mathbf{h}$	$\mathbf{g}$	$k$
0, 6	-.0151449638228338	-.0764119740848740	0, 4
1, 5	-.0700747935660952	-.3535533905932738	1, 3
2, 4	.3686983544161076	.8599307293562955	2
3	.8472563683187380		
$k$	$\tilde{\mathbf{h}}$	$\tilde{\mathbf{g}}$	$k$
1, 5	-.0764119740848740	.0151449638228338	-1, 5
2, 4	.3535533905932738	-.0700747935660952	0, 4
3	.8599307293562955	-.3686983544161076	1, 3
		.8472563683187380	2

Although there are no striking differences performance-wise, we have listed some additional BFBs here for additional reference.

### B1. BFB 7/5 with Condition EP1

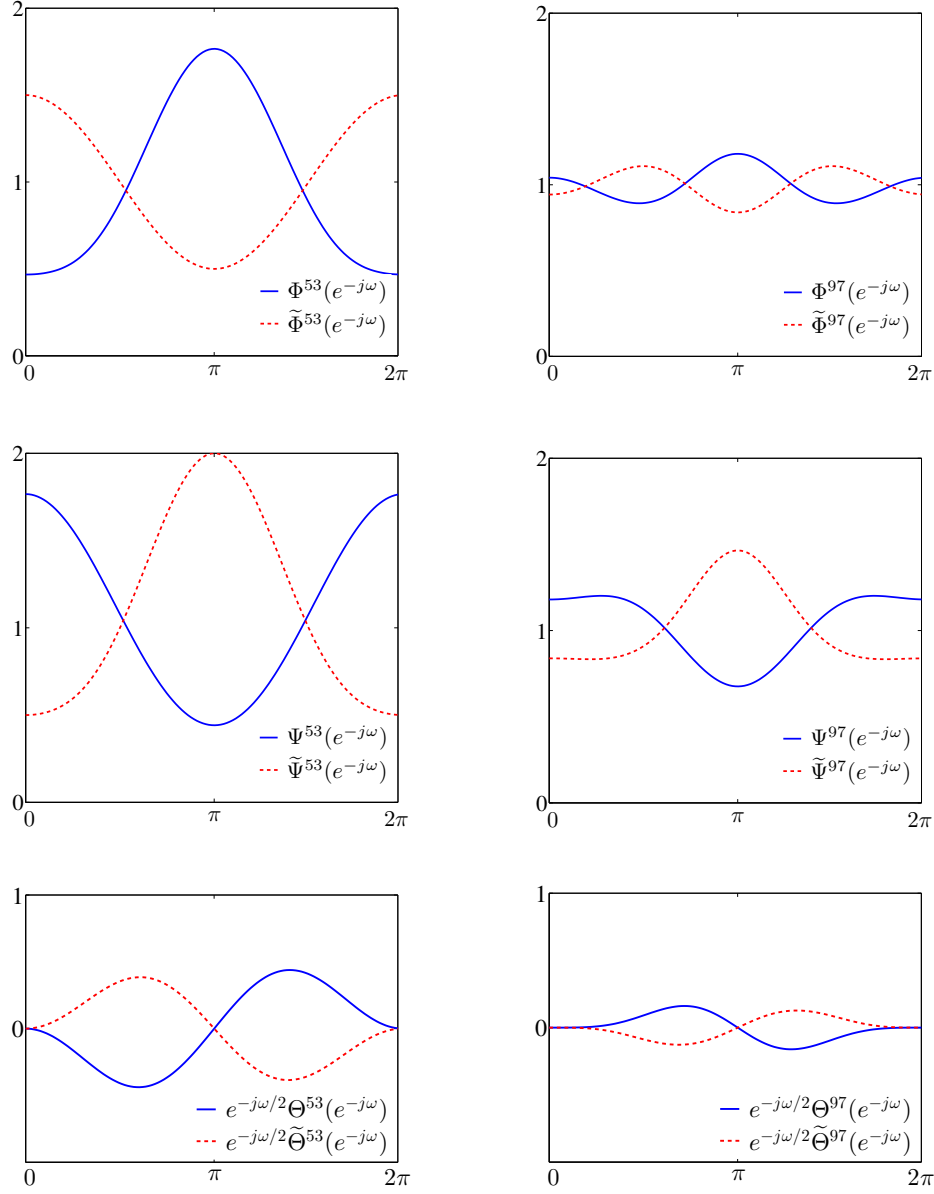


Figure 11. Plots of Euler-Frobenius polynomials  $\Phi^{53}$  and  $\tilde{\Phi}^{53}$ ,  $\Phi^{97}$  and  $\tilde{\Phi}^{97}$ ,  $\Psi^{53}$  and  $\tilde{\Psi}^{53}$ ,  $\Psi^{97}$  and  $\tilde{\Psi}^{97}$ ,  $e^{j\omega/2}\Theta^{53}(e^{-j\omega})$  and  $e^{j\omega/2}\tilde{\Theta}^{53}(e^{-j\omega})$ , and  $e^{j\omega/2}\Theta^{97}(e^{-j\omega})$  and  $e^{j\omega/2}\tilde{\Theta}^{97}(e^{-j\omega})$ .

With  $\tilde{b}$  in (72), the BFB 7/5 with Condition EP1 is created and listed in Table 25. Weights of the BFB 7/5 with Condition EP1 are in Table 26.

### B2. BFB 7/5 with Condition EP2

With  $\tilde{b}$  in (73), the BFB 7/5 with Condition EP2 is listed in Table 27. Weights of the BFB 7/5 with Condition EP2 are in Table 28.

### B3. BFB 7/5 with Condition EP3

With  $\tilde{b}$  in (74), the BFB 7/5 with Condition EP3 is listed in Table 29. Weights of the BFB 7/5

Table 26. Weights of BFB 7/5 with Condition EP1

Weights	$\mathbf{h}$	$\tilde{\mathbf{h}}$	Weights
$w_{0,0}$	1.0000000000000000	1.0011584388583453	$\tilde{w}_{0,0}$
$w_{0,1}$	1.0011584388583453	1.0000000000000000	$\tilde{w}_{0,1}$
$w_{1,0}$	1.0068238600793053	.9951317153039584	$\tilde{w}_{1,0}$
$w_{1,1}$	.9945841422399645	1.0086122849043330	$\tilde{w}_{1,1}$
$w_{2,0}$	1.0100895003967167	.9920412683722906	$\tilde{w}_{2,0}$
$w_{2,1}$	1.0048421375340930	.9995308201053070	$\tilde{w}_{2,1}$
$w_{3,0}$	1.0112494712026609	.9908412812103105	$\tilde{w}_{3,0}$
$w_{3,1}$	1.0101396571595314	.9944741248265543	$\tilde{w}_{3,1}$

Table 27. BFB 7/5 with Condition EP2

$k$	$\mathbf{h}$	$\mathbf{g}$	$k$
0, 6	-.0151486519354670	-.0761025218356459	0, 4
1, 5	-.0703768695900569	-.3535533905932738	1, 3
2, 4	.3687020425287408	.8593118248578394	2
3	.8478605203666614		
$k$	$\tilde{\mathbf{h}}$	$\tilde{\mathbf{g}}$	$k$
1, 5	-.0761025218356459	.0151486519354670	-1, 5
2, 4	.3535533905932738	-.0703768695900569	0, 4
3	.8593118248578394	-.3687020425287408	1, 3
		.8478605203666614	2

with Condition EP3 are in Table 30.

#### B4. BFB 9/7 with Condition EP3

Similar to the BFB 9/7 with Condition EP1 & Condition EP2 in Section 5, BFB 9/7 with Condition EP3 is tabulated in Table 31, and weights of the BFB 9/7 with Condition EP3 are in Table 32.

#### B5. BFB 9/7 with Condition EP4

Meanwhile, BFB 9/7 with Condition EP4 is in Table 33, and weights of the BFB 9/7 with Condition EP4 are in Table 34.

#### B6. BFB 11/9 with Condition EP4

Due to their minor differences, we omit the BFB 11/9's with Condition EP1 & Condition EP2 and list only the BFB 11/9 with Condition EP4 here.

With (95), the BFB 11/9 with Condition EP4 is in Table 35, and weights of the BFB 11/9 with Condition EP4 are in Table 36.

#### B7. BFB 13/11 with Condition EP3

With (98) and (3), the BFB 13/11 with Condition EP3 is in Table 37, and weights of the BFB 13/11 with Condition EP3 are in Table 38.

Table 28. Weights of BFB 7/5 with Condition EP2

Weights	<b>h</b>	<b><math>\tilde{h}</math></b>	Weights
$w_{0,0}$	1.0011146251836722	1.0000000000000000	$\tilde{w}_{0,0}$
$w_{0,1}$	1.0000000000000000	1.0011146251836722	$\tilde{w}_{0,1}$
$w_{1,0}$	1.0083778820416620	.9935179995006257	$\tilde{w}_{1,0}$
$w_{1,1}$	.9951958546531894	1.0078431000042233	$\tilde{w}_{1,1}$
$w_{2,0}$	1.0117926119215717	.9902737777554436	$\tilde{w}_{2,0}$
$w_{2,1}$	1.0061697083456300	.9979907125132796	$\tilde{w}_{2,1}$
$w_{3,0}$	1.0129995565062208	.9890259382163199	$\tilde{w}_{3,0}$
$w_{3,1}$	1.0117128639350284	.9926686881641895	$\tilde{w}_{3,1}$

Table 29. BFB 7/5 with Condition EP3

$k$	<b>h</b>	<b>g</b>	$k$
0, 6	-.0151468900092339	-.0762542300151167	0, 4
1, 5	-.0702286852630524	-.3535533905932738	1, 3
2, 4	.3687002806025077	.8596152412167809	2
3	.8475641517126523		
$k$	<b>h</b>	<b><math>\tilde{g}</math></b>	$k$
1, 5	-.0762542300151167	.0151468900092339	-1, 5
2, 4	.3535533905932738	-.0702286852630524	0, 4
3	.8596152412167809	-.3687002806025077	1, 3
		.8475641517126523	2

### APPENDIX III

#### Even-Length BFBs

Although the odd-length BFB filters with certain EP conditions are emphasized and constructed, even-length BFBs are exhibiting eminence in some other applications (Balasingham et al., 1997; Muthuvel and Makur, 2000; Zanjani et al., 2006; Tay, 2008). For completeness, we include in this appendix the construction of even-length BFB, with Condition EP3 in particular.

Similar to (49)–(50) and to be more specific, we write

$$H(z) = \left(\frac{1+z}{2}\right)^{2m-1} S_{2m}(z), \quad (130)$$

$$\tilde{H}(z) = \left(\frac{1+z}{2}\right)^{2m-1} \tilde{S}_{2m}(z), \quad (131)$$

where, again,  $S_{2m}$  and  $\tilde{S}_{2m}$  are reciprocal polynomials of exact degree  $2m$  that satisfy

$$(1+z) \nmid S_{2m}(z), \quad \tilde{S}_{2m}(z);$$

$$S_{2m}(1) = \tilde{S}_{2m}(1) = 1.$$

Consequently, the filterbanks will be CDF  $4m/4m$ , i.e., both lowpass and highpass filters are with linear phases and both have the *same* even length  $4m$ . Moreover, all wavelets will have

Table 30. Weights of BFB 7/5 with Condition EP3

Weights	$\mathbf{h}$	$\tilde{\mathbf{h}}$	Weights
$w_{0,0}$	1.0005677781225810	1.0005677781225810	$\tilde{w}_{0,0}$
$w_{0,1}$	1.0005677781225810	1.0005677781225810	$\tilde{w}_{0,1}$
$w_{1,0}$	1.0076152978003301	.9943086876100272	$\tilde{w}_{1,0}$
$w_{1,1}$	.9948954892055626	1.0082199181408479	$\tilde{w}_{1,1}$
$w_{2,0}$	1.0109567818589060	.9911396873261831	$\tilde{w}_{2,0}$
$w_{2,1}$	1.0055179699539433	.9987451146284400	$\tilde{w}_{2,1}$
$w_{3,0}$	1.0121406356051454	.9899152340376341	$\tilde{w}_{3,0}$
$w_{3,1}$	1.0109404797885825	.9935529244813030	$\tilde{w}_{3,1}$

Table 31. BFB 9/7 with Condition EP3

$k$	$\mathbf{h}$	$\mathbf{g}$	$k$
0, 8	.0010156505199965	.0085338086354344	0, 6
1, 7	-.0086621451841133	-.0727820130233624	1, 5
2, 6	-.0736653767141652	-.3620871992287082	2, 4
3, 5	.3622155357773871	.8526708072332723	3
4	.8524062335748848		
$k$	$\tilde{\mathbf{h}}$	$\tilde{\mathbf{g}}$	$k$
1, 7	-.0085338086354344	.0010156505199965	-1, 7
2, 6	-.0727820130233624	.0086621451841133	0, 6
3, 5	.3620871992287082	-.0736653767141652	1, 5
4	.8526708072332723	-.3622155357773871	2, 4
		.8524062335748848	3

$2m - 1$  VM. The integer  $K$  in (12) or (18)–(19) is  $2m$ . Again, with  $t$  defined in (53) and similar to (54)–(55),  $H$  and  $\tilde{H}$  in (130)–(131) can be re-written as

$$H(z) = z^{2m-1} \frac{1+z}{2} (1-t)^{m-1} F_m(t), \quad (132)$$

$$\tilde{H}(z) = z^{2m-1} \frac{1+z}{2} (1-t)^{m-1} G_m(t), \quad (133)$$

for  $F_m$  and  $G_m$  of exact degrees  $m$  and satisfying

$$(1-t)^{2m-1} F_m(t) G_m(t) + t^{2m-1} F_m(1-t) G_m(1-t) = 1, \quad t \in [0, 1]; \quad (134)$$

$$F_m(0) = G_m(0) = 1. \quad (135)$$

Hence, it follows from (Lian, 2001) that  $F_m G_m$  must have the form

$$F_m(t) G_m(t) = \sum_{k=0}^{2m-2} \binom{2m-2+k}{k} t^k + C_0 t^{2m-1} (1-2t), \quad (136)$$

for some constant  $C_0$ , which is determined by one of the four EP conditions. With  $\varepsilon = 1$ ,  $G$  and  $\tilde{G}$  in (18) and (19) are

$$G(z) = \tilde{H}(-z), \quad (137)$$

$$\tilde{G}(z) = H(-z). \quad (138)$$

Table 32. Weights of BFB 9/7 with Condition EP3

Weights	<b>h</b>	<b>h̃</b>	Weights
$w_{0,0}$	1.0000018798175388	1.0000018798175388	$\tilde{w}_{0,0}$
$w_{0,1}$	1.0000018798175388	1.0000018798175388	$\tilde{w}_{0,1}$
$w_{1,0}$	.9990960702729141	1.0009083272092260	$\tilde{w}_{1,0}$
$w_{1,1}$	1.0009124638458001	.9991002095131160	$\tilde{w}_{1,1}$
$w_{2,0}$	.9986848067419229	.9995115651108249	$\tilde{w}_{2,0}$
$w_{2,1}$	1.0013202826100966	1.0005006137345623	$\tilde{w}_{2,1}$
$w_{3,0}$	.9985361059398271	1.0014696499812666	$\tilde{w}_{3,0}$
$w_{3,1}$	.9988374515320433	1.0011748731599354	$\tilde{w}_{3,1}$

Table 33. BFB 9/7 with Condition EP4

$k$	<b>h</b>	<b>g</b>	$k$
0, 8	.0010156505153183	.0085338088016166	0, 6
1, 7	-.0086621450090733	-.0727820133051835	1, 5
2, 6	-.0736653764313465	-.3620871993948904	2, 4
3, 5	.3622155356023471	.8526708077969146	3
4	.8524062330186039		
$k$	<b>h̃</b>	<b>g̃</b>	$k$
1, 7	-.0085338088016166	.0010156505153183	-1, 7
2, 6	-.0727820133051835	.0086621450090733	0, 6
3, 5	.3620871993948904	-.0736653764313465	1, 5
4	.8526708077969146	-.3622155356023471	2, 4
		.8524062330186039	3

Observe that if  $(\phi_{4m,4m}^{EP1}, \psi_{4m,4m}^{EP1})$  and  $(\tilde{\phi}_{4m,4m}^{EP1}, \tilde{\psi}_{4m,4m}^{EP1})$  constitute a biorthogonal system, then  $\phi_{4m,4m}^{EP2} = \tilde{\phi}_{4m,4m}^{EP1}$  and  $\psi_{4m,4m}^{EP2} = \tilde{\psi}_{4m,4m}^{EP1}$ . In other words, BFBs  $4m/4m$  with Condition EP1 and BFBs  $4m/4m$  with Condition EP2 are constructed simultaneously mainly due to the fact that all filters have the same length  $4m$ .

As a demonstrative example, we set  $m = 3$  and construct the BFB 12/12 with Condition EP3. Write  $F_3$  and  $G_3$  as

$$F_3(t) = 1 + a_1 t + a_2 t^2 + a_3 t^3,$$

$$G_3(t) = 1 + b_1 t + b_2 t^2 + b_3 t^3.$$

Then (134)–(136) and Condition EP3 lead to

$$a_1 = 1.3337433665494807, \quad a_2 = 5.4443351973811674,$$

$$a_3 = 14.0786114247078130; \quad b_1 = 3.6662566334505193,$$

$$b_2 = 4.6658193376861715, \quad b_3 = -5.2619470479918829;$$

$$C_0 = 37.0404539130330370.$$



Table 34. Weights of BFB 9/7 with Condition EP4

Weights	<b>h</b>	<b>h̃</b>	Weights
$w_{0,0}$	1.0000018785261557	1.0000018811071500	$\tilde{w}_{0,0}$
$w_{0,1}$	1.0000018811071500	1.0000018785261557	$\tilde{w}_{0,1}$
$w_{1,0}$	.9990960683347463	1.0009083291495102	$\tilde{w}_{1,0}$
$w_{1,1}$	1.0009124632001835	.9991002101510407	$\tilde{w}_{1,1}$
$w_{2,0}$	.9986848045660166	1.0013202847915708	$\tilde{w}_{2,0}$
$w_{2,1}$	.9995115634080709	1.0005006154313355	$\tilde{w}_{2,1}$
$w_{3,0}$	.9985361036863355	1.0014696522420125	$\tilde{w}_{3,0}$
$w_{3,1}$	.9988374494307633	1.0011748752591805	$\tilde{w}_{3,1}$

Table 35. BFB 11/9 with Condition EP4

$k$	<b>h</b>	<b>g</b>	$k$
0, 10	.0006498856781080	.0011905000307570	0, 8
1, 9	.0360931817123812	.0661176809801392	1, 7
2, 8	-.0242203237025032	-.0486090144349880	2, 6
3, 7	-.1005257125375647	-.4196710715734130	3, 5
4, 6	.3771238286176690	.8019438099950095	4
5	.8359718428369145		
$k$	<b>h̃</b>	<b>g̃</b>	$k$
1, 9	.0011905000307570	-.0006498856781080	-1, 9
2, 8	-.0661176809801392	.0360931817123812	0, 8
3, 7	-.0486090144349880	.0242203237025032	1, 7
4, 6	.4196710715734130	-.1005257125375647	2, 6
5	.8019438099950095	-.3771238286176690	3, 5
		.8359718428369145	4

Table 36. Weights of BFB 11/9 with Condition EP4

Weights	<b>h</b>	<b>h̃</b>	Weights
$w_{0,0}$	1.0072840523965583	1.0088330936461765	$\tilde{w}_{0,0}$
$w_{0,1}$	1.0088330936461765	1.0072840523965583	$\tilde{w}_{0,1}$
$w_{1,0}$	.9530846410106563	1.0664856176370199	$\tilde{w}_{1,0}$
$w_{1,1}$	1.0843858100807528	.9747330034352886	$\tilde{w}_{1,1}$
$w_{2,0}$	.9291943194242402	1.0915900107533816	$\tilde{w}_{2,0}$
$w_{2,1}$	.9947688827217231	1.0616741591490110	$\tilde{w}_{2,1}$
$w_{3,0}$	.9217294743698444	1.0990277801836811	$\tilde{w}_{3,0}$
$w_{3,1}$	.9518735266152172	1.1025443025356975	$\tilde{w}_{3,1}$

Hence, (132)–(133) yields

$$\begin{aligned}
h_0 = h_{11} &= -.0097217593829114, & h_1 = h_{10} &= .0247597528872896, \\
h_2 = h_9 &= .0489108688744086, & h_3 = h_8 &= -.1087743617414911, \\
h_4 = h_7 &= .0488653797296422, & h_5 = h_6 &= .7030669008196096;
\end{aligned}$$

Table 37. BFB 13/11 with Condition EP3

$k$	$\mathbf{h}$	$\mathbf{g}$	$k$
0, 12	.0078836658313995	.0170492651873219	0, 10
1, 11	.0025213736454515	.0054527384641817	1, 9
2, 10	.0154219421943901	.0160277522896776	2, 8
3, 9	-.0287769207330297	-.0677737019116951	3, 7
4, 8	-.0866780132051877	-.3866304080702732	4, 6
5, 7	.3798089376808520	.8317487080815741	5
6	.8338515915453438		
$k$	$\tilde{\mathbf{h}}$	$\tilde{\mathbf{g}}$	$k$
1, 11	-.0170492651873219	.0078836658313995	-1, 11
2, 10	.0054527384641817	-.0025213736454515	0, 10
3, 9	-.0160277522896776	.0154219421943901	1, 9
4, 8	-.0677737019116951	.0287769207330297	2, 8
5, 7	.3866304080702732	-.0866780132051877	3, 7
6	.8317487080815741	-.3798089376808520	4, 6
		.8338515915453438	5

Table 38. Weights of BFB 13/11 with Condition EP3

Weights	$\mathbf{h}$	$\tilde{\mathbf{h}}$	Weights
$w_{0,0}$	1.0011132049134615	1.0011132049134615	$\tilde{w}_{0,0}$
$w_{0,1}$	1.0011132049134615	1.0011132049134615	$\tilde{w}_{0,1}$
$w_{1,0}$	.9706153388077445	1.0322355935379490	$\tilde{w}_{1,0}$
$w_{1,1}$	1.034072922243983	.9723761734666035	$\tilde{w}_{1,1}$
$w_{2,0}$	.9496103586911090	1.0544853745092700	$\tilde{w}_{2,0}$
$w_{2,1}$	.9937697324329497	1.0122158919865541	$\tilde{w}_{2,1}$
$w_{3,0}$	.9423122148861941	1.0624985209271279	$\tilde{w}_{3,0}$
$w_{3,1}$	.9585048727295536	1.0482316824973282	$\tilde{w}_{3,1}$

and

$$\begin{aligned}\tilde{h}_0 = \tilde{h}_{11} &= .0036335531639449, & \tilde{h}_1 = \tilde{h}_{10} &= .0092540737636692, \\ \tilde{h}_2 = \tilde{h}_9 &= -.0457869346277827, & \tilde{h}_3 = \tilde{h}_8 &= -.1107089552735895, \\ \tilde{h}_4 = \tilde{h}_7 &= .1652490973141165, & \tilde{h}_5 = \tilde{h}_6 &= .6854659468461891;\end{aligned}$$

and, by using (137)–(138),

$$g_k = (-1)^k \tilde{h}_k, \quad \tilde{g}_k = (-1)^k h_k, \quad k = 0, \dots, 11.$$

The initial level weights are

$$w_{0,0} = w_{0,1} = \tilde{w}_{0,0} = \tilde{w}_{0,1} = 1.0232451703981401.$$

Again, by using (109)–(112), the Riesz bounds for  $\{\phi_{12,12}^{EP3}(\cdot - k)\}_{k \in \mathbb{Z}}$  and  $\{\tilde{\phi}_{12,12}^{EP3}(\cdot - k)\}_{k \in \mathbb{Z}}$  are found in the following

$$\begin{aligned}.8440350201656507 &\leq \Phi_{12,12}^{EP3}(e^{-j\omega}) \leq 1.2136551093739243, \\ .8046326219081530 &\leq \tilde{\Phi}_{12,12}^{EP3}(e^{-j\omega}) \leq 1.1673948582780465,\end{aligned}$$

where  $\Phi_{12,12}^{EP3}$  and  $\tilde{\Phi}_{12,12}^{EP3}$  are the Euler-Frobenius polynomials of  $\phi_{12,12}^{EP3}$  and  $\tilde{\phi}_{12,12}^{EP3}$ , as introduced in (104) or (105). In addition, the corresponding refinable functions  $\phi_{12,12}^{EP3}$  and  $\tilde{\phi}_{12,12}^{EP3}$  have Hölder exponents 1.0943 and 2.1108, i.e.,  $\phi_{12,12}^{EP3} \in C^{1.0943}$  and  $\tilde{\phi}_{12,12}^{EP3} \in C^{2.1108}$ .

## REFERENCES

- Abdelnour, A. F. and Selesnick, I. W. (2004). Symmetric nearly orthogonal and orthogonal nearly symmetric wavelets. *The Arabian Journal for Science and Engineering*, 29(2C):3–16.
- Antonini, M., Barlaud, M., Mathieu, P., and Daubechies, I. (1992). Image coding using wavelet transform. *IEEE Transactions on Image Processing*, 1(2):205–220.
- Balasingham, I., Ramstad, T. A., and Lervik, J. M. (1997). Survey of odd and even length filters in tree-structured filter banks for subband image compression. In *Proceedings of the International Conference on Acoustics, Speech, and Signal Processing*, volume 4, pages 3073–3076, Munich, Germany.
- Cohen, A., Daubechies, I., and Feauveau, J.-C. (1992). Biorthogonal bases of compactly supported wavelets. *Communications on Pure and Applied Mathematics*, 45(5):485–560.
- Daubechies, I. (1988). Orthonormal bases of compactly supported wavelets. *Communications on Pure and Applied Mathematics*, 41(7):909–996.
- Daubechies, I. (1992). *Ten Lectures on Wavelets*. Society for Industrial and Applied Mathematics, Philadelphia, PA.
- de Saint-Martin, F. M., Siohan, P., and Cohen, A. (1999). Biorthogonal filterbanks and energy preservation property in image compression. *IEEE Transactions on Image Processing*, 8(2):168–178.
- Hamou, A. K. and El-Sakka, M. R. (2003). Wavelet-filter performance evaluation for digital images. In *IEEE CCECE Canadian Conference on Electrical and Computer Engineering*, volume 3, pages 2075–2078, Montreal, Quebec, Canada.
- Le Gall, D. and Tabatabai, A. (1988). Sub-band coding of digital images using symmetric short kernel filters and arithmetic coding techniques. In *Proceedings of the International Conference on Acoustics, Speech, and Signal Processing*, volume 2, pages 761–764, New York, NY.
- Lian, J. and Wang, Y. (2014). Energy preserving QMF for image processing. *IEEE Transactions on Image Processing*, 23(7):3166–3178.
- Lian, J.-A. (2001). Polynomial identities of Bézout type. In Lyche, T., Kopotun, K., and Neamtu, M., editors, *Trends in Approximation Theory*, pages 243–252. Vanderbilt University Press, Nashville, TN.
- Muthuvel, A. and Makur, A. (2000). Design of two-channel linear-phase fir pr filter banks with even length filters using convolution matrices. *IEEE Transactions on Circuits and Systems Part II: Analog & Digital Signal Processing*, 47(12):1413–1418.
- Said, A. and Pearlman, W. A. (1996). A new, fast, and efficient image codec based on set

- partitioning in hierarchical trees. *IEEE Transactions on Circuits and Systems for Video Technology*, 6(3):243–250.
- Tay, D. B. H. (2008). ETHFB: A new class of even-length biorthogonal wavelet filters for hilbert pair design. *IEEE Transactions on Circuits and Systems*, 55(6):1580–1588.
- Usevitch, B. E. (1996). Optimal bit allocation for biorthogonal wavelet coding. In *Proceedings of the IEEE Data Compression Conference*, pages 387–395, Snowbird, UT.
- Usevitch, B. E. (2001). A tutorial on modern lossy wavelet image compression: Foundations of JPEG 2000. *IEEE Signal Processing Magazine*, 18(5):22–35.
- Wei, D., Tian, J., Wells, Jr., R. O., and Burrus, C. S. (1998). A new class of biorthogonal wavelet system for image transform coding. *IEEE Transactions on Image Processing*, 7(7):1000–1013.
- Woods, J. W. and Naveen, T. (1992). A filter based bit allocation scheme for subband compression of hdtv. *IEEE Transactions on Image Processing*, 1(3):436–440.
- Yang, X., Ramchandran, K., and Moulin, P. (1998). Optimization of high-energy-compaction, nearly-orthonormal, linear-phase filter banks. In *Proceedings of the IEEE International Symposium on Circuits and Systems*, volume 5, pages 106–109, Monterey, CA.
- Zanjani, S. M. M., Fakhraie, S. M., Shoaie, ., and Salehi, M. E. (2006). Design of fir filters using identical subfilters of even length. In *2006 International Conference on Microelectronics*, pages 83–86, Dhahran, Saudi Arabia.